AD-A166 089 INVESTIGATION OF BASIC CHARACTERISTICS OF LASER HEATING IN THERMOLUMINESC..(U) WASHINGTON STATE UNIV PULLMAN DEPT OF PHYSICS P F BRAUNLICH ET AL. 10 MAR 86 1/1

UNCLASSIFIED N00014-82-K-0529 F/G 20/13 NL

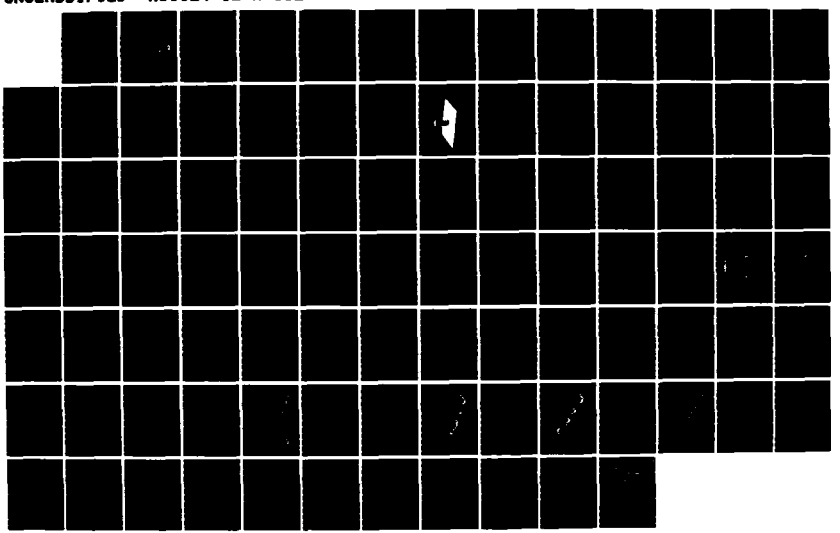

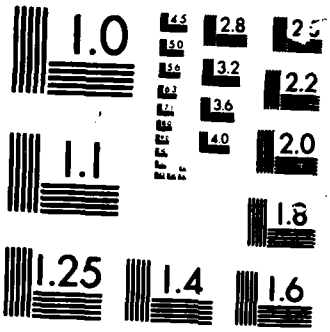

MICROCOPY RESOLUTION TEST CHART

Send to DTIC (1)

AD-A166 089

SECURITY CLASSIFICATION OF THIS PAGE (When Data Entered)

REPORT DOCUMENTATION PAGE		READ INSTRUCTIONS BEFORE COMPLETING FORM
1. REPORT NUMBER	2. GOVT ACCESSION NO.	3. RECIPIENT'S CATALOG NUMBER
4. TITLE (and Subtitle) Investigation of Basic Characteristics of Laser Heating in Thermoluminescence and of Laser-Stimulated Luminescence		5. TYPE OF REPORT & PERIOD COVERED Annual Report 7/15/85 - 7/15/86
		6. PERFORMING ORG. REPORT NUMBER
7. AUTHOR(s) P.I. Peter F. Braunlich		8. CONTRACT OR GRANT NUMBER(s) ONR N00014-82-K-0J29
9. PERFORMING ORGANIZATION NAME AND ADDRESS Department of Physics Washington State University Pullman, WA 99164-2814		10. PROGRAM ELEMENT, PROJECT, TASK AREA & WORK UNIT NUMBERS Task Area: RR011-07-01 Work Unit: NR359-079 Program Element: 61153N
11. CONTROLLING OFFICE NAME AND ADDRESS Office of Naval Research 800 N. Quincy Street Arlington, VA 22217		12. REPORT DATE 3/18/86
		13. NUMBER OF PAGES
14. MONITORING AGENCY NAME & ADDRESS(if different from Controlling Office) Office of Naval Research University District Bldg., Room 422 1107 N.E. 45th Street Seattle, WA 98195		15. SECURITY CLASS. (of this report) Unclassified
		15a. DECLASSIFICATION/DOWNGRADING SCHEDULE
16. DISTRIBUTION STATEMENT (of this Report) Approved for public release, distribution unlimited		
17. DISTRIBUTION STATEMENT (of the abstract entered in Block 20, if different from Report)		
18. SUPPLEMENTARY NOTES		
19. KEY WORDS (Continue on reverse side if necessary and identify by block number) Thermoluminescence, Dosimetry, Laser Heating, Heat Transfer, Uniform Laser Beam Profile, Optically Stimulated Luminescence		
20. ABSTRACT (Continue on reverse side if necessary and identify by block number) See Back		

DTIC ELECTE APR 10 1986 S D E

DTIC FILE COPY

06 4 0 022

DD FORM 1 JAN 73 1473 EDITION OF 1 NOV 65 IS OBSOLETE
S/N 0102-LF-014-6601

SECURITY CLASSIFICATION OF THIS PAGE (When Data Entered)

ABSTRACT

A general solution of the heat diffusion equation is presented for the case of a semi-infinite two-layer system that is heated with a localized cw laser beam of Gaussian or uniform circular intensity profile. As an example, this theory is applied to thin layers of a thermoluminescent material on a substrate. The transient thermoluminescence emission response is calculated and compared with experimental results, illustrating the validity of the solutions. Applications to transient laser heating of oxide-semiconductor sandwiches are discussed.

The theory of heating a semi-infinite two-layer system with a localized CO_2 laser beam of uniform circular intensity profile is also applied to configurations consisting of thin thermoluminescent LiF:Ti,Mg phosphor layers on borosilicate glass substrates. We study thermoluminescence because it serves as a convenient monitor for the temperature distribution and because of its importance in developing the laser heating technique for solid-state dosimetry. Experimental and calculated results are compared in an attempt to completely characterize the thermoluminescence response curves. The two-layer system is heated in two different modes: the laser beam impinges onto (a) the phosphor layer, and (b) the glass substrate. We investigate in detail changes in the thermoluminescence response due to different laser powers and variations in the optical and thermal properties of the samples.

Two optically stimulable phosphors (MgS:Ce,Sm and CaS:Ce,Sm) have been developed with the goal to eventually apply them to imaging of neutron dose distributions. These phosphors exhibit luminescence emission spectra that are different for UV excitation and for IR stimulation, a property necessary for nearly real-time radiography.

INVESTIGATION OF BASIC CHARACTERISTIC OF LASER HEATING IN THERMOLUMINESCENCE AND OF LASER-STIMULATED LUMINESCENCE

Contract No. N00014-82-K-0529

Principal Investigator
P. F. Braunlich

Washington State University
Department of Physics
Pullman, WA 99164-2814

ANNUAL REPORT

7/15/85 - 7/14/86

P. F. BRAUNLICH
A. ABTAHI
P. KELLY
M. RUNKEL

MARCH 18, 1986

WSU PROJECT NO. 0112

RESEARCH GOALS

The purpose of this research effort is the investigation of the basic characteristics of two differnt types of laser-stimulated luminescence phenomena in view of potential applications in the dosimetry of ionizing radiation and of radiation imaging.

The first of these, laser-heated thermoluminescence, was the main subject of research in the contract period from 7-15-83 through 3-15-86. A study of the potential use of optically stimulated luminescence for real-time imaging of neutron dose distributions has been phased in since 5-25-86.

The heat transfer mechnanism from a CO laser beam, having a circular uniform intensity profile, to a semi-infinite thin thermoluminescence phosphor layer and the resulting luminescence response has been studied in detail. Experimental and computational methods were developed for the chacterization of a given thermoluminescence dosimeter configuration. All its relevant optical and thermal properties can be determined by these methods. Based on this knowledge, the expected thermoluminescence response can be computer-simulated as a function of a number of experimental parameters. This in turn provides a tool to optimize the dosimeter design for applications in dosimetry.

Initial experiments are discussed which we performed with a group of Ce/Sm co-doped magnesium and calcium sulphides that can be stimulated with 1.064 um photons from a Nd:YAG laser. The goal is to develop phosphors that exhibit distinctly differnt luminescence emission spectra during excitation with ionizing radiation as compared to those emitted during infra-red stimulation. This characteristic property is essential for real-time or nearly real-time radiographic imaging.

List of Contents

TRANSIENT TEMPERATURE RESPONSE OF A TWO LAYER SYSTEM HEATED WITH A LOCALIZED LASER BEAM

by

Abdollah Abtahi and Peter F. Braunlich
Department of Physics
Washington State University
Pullman, WA 99164-2814

and

Paul Kelly
Division of Microstructural Sciences
National Research Council
Ottawa, Canada, K1A OR6

ABSTRACT

A general solution of the heat diffusion equation is presented for the case of a semi-infinite two-layer system that is heated with a localized cw laser beam of Gaussian or uniform circular intensity profile. As an example, this theory is applied to thin layers of a thermoluminescent material on a substrate. The transient thermoluminescence emission response is calculated and compared with experimental results, illustrating the validity of the solutions. Applications to transient laser heating of oxide-semiconductor sandwiches are discussed.

INTRODUCTION

The interest in heating semi-infinite slabs with localized laser beams stems from the application of laser heating in thermoluminescence dosimetry, which recently has received considerable attention [1-5]. The early work in this field was restricted to the use of cw CO_2 laser beams having Gaussian intensity profiles. The theoretical approach taken for the calculations of the thermoluminescence (TL) response of a thin TL layer on a glass substrate assumed that the TL layer thickness is negligibly small compared to that of the substrate. All thermal properties of the sample were assumed to be due to the substrate alone. Only the reflectivity and absorptance, due to modification of the glass substrate by the thin TL layer, were taken into account. The agreement between experimental TL responses and calculated ones was satisfactory for a number of layer configurations consisting of LiF:Ti,Mg powder (Harshaw/Filtrol TLD-100) on borosilicate glass [5].

For practical applications of laser stimulated thermoluminescence in dosimetry it became apparent, however, that Gaussian beam profiles impose unnecessary restrictions [6]. We have, therefore, developed the optical technology to produce spatially uniform beam intensity profiles [7] which was modified for uniform circular beams, and we subsequently attempted to calculate the thermoluminescence response functions obtained with such a beam on the basis of the simple one-layer theory presented in Ref. 5. It turned out that this theory did not yield the characteristic TL glow curves measured under these conditions. This failure prompted us to work out the theory of localized laser beam heating of a two-layer system. It is the purpose of the present paper to present the general solutions of the heat diffusion equation for this case and apply the theory to the same type of thin-layer thermoluminescence dosimetry configuration (LiF;Ti,Mg TL powder on a borosilicate glass substrate) used for the work described in Ref. 5. For completeness we have also recalculated the transient heating and the resulting TL response of this two-layer configuration for Gaussian heating beams. It is perhaps worthwhile to point out that the

solutions described in this paper are of general validity and may well be useful in other fields of endeavor; i.e., laser annealing of semiconductors.

II. SOLUTIONS TO THE HEAT EQUATIONS

The system we consider consists of two layers of material in perfect thermal contact. As an example picture again a thin layer of a thermoluminescent phosphor on a glass substrate or an oxide layer on a semiconductor. Each layer is characterized by its absorption coefficient for the laser photons, μ_i, thermal conductivity k_i, thermal diffusivity, α_i, and thickness, l_i. The index $i = 1,2$ denotes the respective layer and the total thickness is $L = l_1 + l_2$. We also assume that the laser beam impinges along the z-axis perpendicularly to the x,y plane of the two-layer configuration. The laser beam profile is either circular and uniform (Fig. 1) or Gaussian.

The thermal diffusion equation in cylindrical coordinates (ignoring the effect of the finite speed of heat propagation [8]) is given by

$$r^{-1}\partial[rk_i\,\partial T_i(r,z,t)/\partial r]/\partial r + \partial^2 T(r,z,t)/\partial z^2 + g_i(r,z,t) = (k_i/\alpha_i)\partial T_i(r,z,t)/\partial t \qquad (1)$$

We solve it for the following boundary conditions:

1. the two-layer slab is infinite in radial direction and $T(r,z,t) \rightarrow 0$ as $r \rightarrow \infty$;
2. no heat loss occurs at the boundaries; i.e., $\partial T_i/\partial z = 0$ at $z = 0$ $(i = 1)$ and $z = L$ $(i = 2)$;
3. at the interface $(z = l_1)$, $T_1 = T_2$ and $k_1\,\partial T_1/\partial z = k_2\,\partial T_2/\partial/z$.

The initial condition is $T_i(r,z,t) = T_o$; i.e., room temperature, when the laser is turned on at $t = 0$. The temperature $\Delta T_i(r,z,t) = T_i(r,z,t) - T_o$, obtained from Eq. 1, is the actual temperature increase above T_o.

Correcting for reflection loss at the front surface at $z = 0$, the source functions become for $0 \le t \le t_p$ (t_p is the laser pulse length):

$$g_1(r,z,t) = \mu_1(1 - R_1)(P^*/\pi\omega^2)\exp(-\mu_1 z)f(r,\omega) \qquad (2)$$

and

$$g_2(r,z,t) = \mu_2(1 - R_1)(1 - R_2)\,(P^*/\pi\omega^2)\exp[-\mu_1 l_1 - \mu_2(z-l_1)]f(r,\omega) \qquad (3)$$

where $f(r,\omega) = H(\omega-r)$ for the uniform beam and $f(r,\omega) = \exp(-r^2/\omega^2)$ for the Gaussian beam. P^* is the total laser power (not the power density) incident on the front surface, H the Heaviside step function, R_i the reflectivity layer i, and ω the radius of the uniform circular beam or the 1/e half-width for the Gaussian beam.

We solve Eq. (1) with the initial and boundary conditions given above by the Green's function technique [9]. The general solution, written compactly, is then:

$$\Delta T_i(r,z,t) = \int_0^t d\tau \int_0^\infty r'dr'[(\alpha_1/k_1)\int_0^{l_1} dz' G_{i1}(r,z,t/r',z',\tau)g_1(r',z',\tau) +$$

$$(\alpha_2/k_2)\int_{l_1}^{L} dz' G_{i2}(r,z,t/r',z',\tau)g_2(r',z',\tau)] \qquad (4)$$

$$G_{ij} = (k_j/\alpha_j)\int_0^\infty (\gamma_i d\gamma_i/\alpha_i)\exp[-(\gamma_i^2 + \eta_i^2)(t-\tau)]J_0(\gamma_i r/\sqrt{\alpha_i})\,J_0(\gamma_j r/\sqrt{\alpha_j})$$
$$[x_i(z)x_j(z')]/N \qquad (5)$$

$$N = \sum_{i=1}^{2} k_i l_i/2\alpha_i[1 + \sin 2\theta_i/2\theta_i]/\cos^2(\theta_i) \quad \text{where} \quad \theta_i = \xi_i l_i/\sqrt{\alpha_i} \qquad (6)$$

$$x_i(z) = \begin{cases} \cos(\xi_1 z/\sqrt{\alpha_1})/\cos(\xi_1 l_1/\sqrt{\alpha_1}) & \text{for } i = 1 \\ \cos(\xi_2(L-z)/\sqrt{\alpha_2})/\cos(\xi_2 l_2/\sqrt{\alpha_2}) & \text{for } i = 2 \end{cases} \qquad (7)$$

From the boundary conditions at the interface we have

$$\gamma_1/\sqrt{\alpha_1} = \gamma_2/\sqrt{\alpha_2} = \beta, \qquad (8)$$

$$\sum_{i=1}^{2} k_i\xi_i/\sqrt{\alpha_i}\,\tan(\xi_i l_i/\sqrt{\alpha_i}) = 0 \qquad (9)$$

and

$$\xi_2^2 = \xi_1^2 + \beta^2(\alpha_1 - \alpha_2)\,. \tag{10}$$

The rise in temperature then becomes

$$\begin{aligned}\Delta T_i(r,z,t) = {} & [(1-R_1)P^*/\pi\omega^2 N] \int_0^t d\tau \int_0^\infty r'dr' \int_0^\infty \beta d\beta \exp[\alpha_i\beta^2(t-\tau)]J_0(\beta r)\, x \\ & J_0(\beta r')f(r',\omega)\, x_i(z) \exp[-\xi_i^2(t-\tau)]\{\mu_1^2 \exp(-\mu_1 l_1) \\ & [\exp(\mu_1 l_1) + (\xi_1/\mu_1\sqrt{\alpha_1})\sin(\xi_1 l_1/\sqrt{\alpha_1}) - \\ & \cos(\xi_1 l_1/\sqrt{\alpha_1})]/[(\mu_1^2+\xi_1^2/\alpha_1) \\ & \cos(\xi_1 l_1/\sqrt{\alpha_1})] + (1-R_2)/\mu_2^2 \\ & \exp(-\mu_1 l_1)[\cos(\xi_2 l_2/\sqrt{\alpha_2}) + (\xi_2/\mu_2\sqrt{\alpha})\sin(\xi_2 l_2/\sqrt{\alpha_2}) - \\ & \exp(-\mu_2 l_2)]/[(\mu_2^2 + \xi_2^2/\alpha_2)\cos(\xi_2 l_2/\sqrt{\alpha_2})]\}. \end{aligned} \tag{11}$$

This general solution can be simplified for all those two-layer structures for which one of the layers is much thinner than the other one. As we will show below in several examples, the spatio-temperal temperature distribution of such a configuration can be calculated by assuming $\alpha_1 = \alpha_2 = \alpha$. This assumption entails that the general form of the solution is maintained in regards to the deposition of the laser photons according to the absorption coefficients μ_1 and μ_2, however, that the thermal diffusion is governed mainly by the thicker one of the two layers. Lateral heat diffusion in the thinner of the two layers is negligible. Instead, lateral heating in this layer occurs via diffusion in the thicker layer with heat transport across the interface into the thinner layer. For this case the integration over β and r' in Eq. (11) is readily carried out, yielding

$$\Delta T_i(r,z,t) = (BP^*/\omega^2) \int_0^t d\tau\, Q(t-\tau)\{1 + [(1 - R_1)/\pi B]$$

$$\sum_{m=1}^{\infty} \exp(-\mu_1 l_1)[\exp(-\mu_1 l_1)\cos(\eta_m l_1) + (\eta_m/\mu_1)\sin(\eta_m l_1)]/$$

$$[N_m(1 + \eta_m^2/\mu_1^2)\cos(\eta_m/\mu_1 l_1)] + (1 - R_2)$$

$$\exp(-\mu_1 l_1)[\cos(\eta_m l_2) + (\eta_m/\mu_2)\sin(\eta_m l_2) - \exp(-\mu_2 l_2]/$$

$$[N_m(1 + \eta_m^2/\mu_2^2)\cos(\eta_m l_2)]\}x_i(z)\exp[-\alpha\eta_m^2(t-\tau)] \qquad (12)$$

with $Q(t) = P(\omega/\sqrt{2\alpha t}, r/\sqrt{2\alpha t})$ for uniform circular beam or $\exp(r^2/(\omega^2 + 4\alpha t))/[1 + (4\alpha t/\omega^2)]$ for Gaussian beam profile, where $P(\omega,r) = \int_0^{\omega} \omega' d\omega' I_o(\omega',r)$ x $\exp[-(\omega'^2+r^2)/2]$ is called the circular coverage function [10] or the "p" function [11], $\xi_1/\sqrt{\alpha_1} = \xi_2/\sqrt{\alpha_2} = \eta_m$, $B = (1 - R_1)[1 - (1 - R_2)\exp(-\mu_1 l_1 - \mu_2 l_2) - R_2 \exp(-\mu_1 l_1)]/\pi N_o$ and, from the boundary conditions, the transcendental equation

$$k_1 \tan \eta_m l_1 + k_2 \tan \eta_m l_2 = 0. \qquad (13)$$

where the roots η_m, m = 1,2, . . . are derived in Appendix A.

We illustrate the validity of these results obtained for both the uniform circular and the Gaussian beam by monitoring the thermoluminescence response of a thin TL layer on a glass substrate. We choose as an example a 35-40 μm thick LiF:Ti,Mg layer on a 150 μm thick borosilicate microscope cover slide. The transient temperature distribution is indirectly monitored via the transient thermoluminescence response of the thin active layer to localized laser heating, measured with a photomultiplier. We point out, however, that in this way the spatially integrated TL signal is measured without spatial resolution. Only the temporal evolution of the thermoluminescence signal is monitored. The procedure for calculating the thermoluminescence transient is based on the well-known electron kinetics for this thermoluminescent phosphor (see below).

The absorption coefficient of LiF for 10.6 μm CO_2 laser photons is 40 cm^{-1} and that of glass is very high. Consequently, we have $\mu_1 l_1 << 1$ for the LiF layer and $\mu_2 l_2 >> 1$ for the glass substrate. We have locally heated this structure with laser beams of Gaussian and uniform circular profiles, constant power P^*, and various beam sizes from both sides, that is the active TL layer can either be on top at $z = 0$ or at the bottom at $z = L$, and we have monitored the transient thermoluminescence response in both cases. The transient temperature distributions are readily obtained from Eq. (12) as follows:

a. Case 1: thermoluminescent layer on top of the glass substrate ($\mu_1 l_1 << 1$)

$$\Delta T_1(r,z,t) = (BP^*/\omega^2) \int_0^t d\tau\, Q(r,t-\tau)\{1 + N_o \sum_{m=1}^{\infty} \cos(\eta_m z) \exp[-\alpha\eta_m^2 (t-\tau)]/[N_m(1 + \eta_m^2/\mu_2^2) \cos(\eta_m l_1)]\} \quad (14)$$

b. Case 2: thermoluminescent layer at the bottom of the glass substrate ($\mu_2 l_2 << 1$)

$$\Delta T_2(r,z,t) = (BP^*/\omega^2) \int_0^t d\tau\, Q(r,t-\tau)\{1 + N_o \sum_{m=1}^{\infty} \cos(\eta_m (L-z)) \exp[-\alpha\eta_m^2 (t-\tau)]/[N_m(1 + \eta_m^2/\mu_1^2) \cos(\eta_m l_1) \cos(\eta_m l_2)]\} \quad (15)$$

In Eqs. (14) and (15) we have written $N_o = (1/\alpha) \sum_{i=1}^{a} k_i l_i$ and $N_m = (1/2\alpha) \sum_{i=1}^{a} k_i l_i [1 + (\sin 2\theta_i)/(2\theta_i)]/\cos^2\theta_i$, where $\theta_i = \eta_m l_i$. The calculations were performed with the following values for the thermal conductivities of the two layers:

1. TL layer: $k_1 = 0.0275$ W/Kcm
2. Glass substrate: $k_2 = 0.00942$ W/Kcm.

Both of these values are temperature dependent. The temperature dependence of k_2 for glass is given by $k_2 = 0.00942\ (1 + \sigma\Delta T_i)$ with $\sigma = 0.00222\ K^{-1}$ [12]. This can be

accounted for in our calculations by the method of the Kirchhoff transformation [5]. A "corrected temperature" $T_{Ni} = T_o + \sigma^{-1}[(1 + 2\sigma\Delta T_i)^{1/2} - 1]$ is introduced with the same σ. The temperature dependence of k_1 for LiF does not have to be accounted for. This is so because of the fact that it is only a very thin layer and, as we explained above, lateral heat diffusion is dominated by the thicker glass layer.

The thermal diffusivity, α, assumed to be identical for both layers (see above) requires special attention. According to the glass manufacturer [12] it is slightly temperature dependent as well. It varies from 0.0052 to 0.0057 cm^2/s between 0°C and 100°C respectively, and it is expected to be somewhat higher yet at the highest temperature of 400°C reached in our measurements. We choose not to correct for this small variation in α with T. Instead, we determine an average value for the thermal diffusivity by the best fit of the calculated and the measured thermoluminescence response curves obtained with the uniform circular beam. It turns out that the high temperature decay of this curve is very sensitive to slight variations in α. The best fit in all cases reported on below (including the ones where a Gaussian beam was employed) was obtained with $\alpha = 0.0064$ cm^2/s. This value is consistent with expectation as the peak of the TL response curve occurs at about 250°C, which appears to be a good "average" temperature for which to select a value for the thermal diffusivity.

For computational efficiency, the numerical calculations of Eqs. (14) and (15) start at the lower time limit of $t = 10^{-6}$ s rather than zero. This can be done since for laser powers that are believed to be practical in thermoluminescence dosimetry applications the temperature rise anywhere in the sample during the initial microsecond is always much smaller than the temperature at which any thermoluminescence signal can be detected.

The prefactor $B = (1 - R_1)(1 - R_2)/\pi N_o$ in Eqs. (14) and (15) is measured by the procedure described in detail in Ref. 5. This procedure determines the absorptance and B is, except for a constant factor, the fraction of the laser power absorbed by the two-layer

system. Its measurement automatically includes the reflection on the front surface and the interface. The roots obtained from the boundary condition are derived in Appendix A.

The thermoluminescence glow curves we consider are commonly called peaks 3, 4, and 5. They are sufficiently well described by simple first-order kinetics with attempt-to-escape frequencies of 4×10^{13} s^{-1}, 7.3×10^{15} s^{-1}, and 4×10^{21} s^{-1}, and trap depth of 1.23 eV, 1.54 eV, and 2.17 eV, respectively [13]. Their relative intensities are adjusted to yield the actual glow curve measured with conventional uniform heating. Peaks 1 and 2 are removed by a 10 minute pre-anneal treatment at 100°C. The two-layer configuration is irradiated with ^{60}Co gamma rays to fill the electron traps and exposed to a uniform circular CO_2 laser beam of fixed 6.5 watts power both from the front (active TL layer exposed directly) and from the back (active layer heated via diffusion through the glass substrate, which is exposed to the laser beam). Laser heating generates a time-dependent transient spatial temperature distribution which results in the TL emission response shown in Figs. 2(a) and 2(b), measured without spatial resolution by a photomultiplier detector. As stated above, the one-layer theory does not yield satisfactory agreement with measured thermoluminescence response curves when the heating beam has a uniform circular intensity profile. These curves have a pronounced peak. However, due to lateral diffusion, the thermoluminescence intensity does not vanish completely, when heating is continued indefinitely after peak occurrence. We have compared the simple two-layer theory and the one in which the temperature dependence of the thermal conductivity is taken into account (via the Kirchhoff transformation technique) with experimental results obtained for a fixed laser power of 6.5 watts and a beam radius of $\omega = 0.15$ cm (Figs. 2(a) and 2(b)). The thermal diffusivity chosen was again $\alpha = 0.0064$ cm^2/s (an "average temperature value"). The prefactor B was selected to yield the best fit. It is to be compared with experimental values, determined with the method of Ref. 5, for both front and back heating of $B = 10.7 \pm 25\%$ K-cm^2/J and $B = 6.3 \pm 20\%$ K-cm^2/J, respectively.

The agreement between the measured and the calculated thermoluminescence response curves is very good, confirming the validity of the theoretical approach presented above.

We have carried out a detailed program exploring the thermoluminescence response curves obtained under various experimental conditions for the purpose of characterizing this type of laser heating in dosimetry applications. The results will be presented in a forthcoming publication [14].

Figures 3(a) and 3(b) are families of curves measured for different beam diameters (1/e-widths ω) of the Gaussian laser beam. The previous one-layer approximation [5] yielded a satisfactory fit only by adjusting the prefactor B. With the two-layer heat equation we obtain the curves drawn through the experimental points in Figs. 3(a) and 3(b) in one case without correcting for the temperature dependence of the thermal conductivity and, for comparison, when the temperature dependence is taken into account by the method of the Kirchhoff transformation as described above. Again, the prefactor B had to be adjusted slightly for the best fit. We note that the two-layer theory represents a rather marked improvement of the previous one-layer approximation.

In conclusion, we have presented a general theory of heating two-layer systems with localized laser beams of Gaussian and uniform circular intensity profiles and checked its validity by comparing calculated and measured thermoluminescence response curves obtained with thin-layer TL phosphor structures on glass in a simpler substrate. The theory is well suited for all systems that consist of a thin layer of a given material in perfect contact with a thicker substrate of different optical and thermal properties. In particular, we expect the theory to be applicable to local heating (laser annealing) of thin oxide or epitaxial layers on semiconductor or insulator substrates.

APPENDIX A

In this work we have a poorly absorbing phosphor coating $l_1 = 0.2L$ on a highly absorbing glass slide, $l_2 = 0.8L$ where the total thickness $L = 0.01875$ cm. In this case m distinct roots η_m can be obtained from the transcendental equation $k_1 \tan\theta + k_2 \tan 4\theta = 0$ with $\theta = 0.2\eta_m L$. With $F = 5\pi/L$, $h = 3+2/k$, $k = k_1/k_2$, $D^+ = \{h + [h^2 - (1 + 4/k)]^{1/2}\}^{1/2}$ and $D^- = \{h - [h + (1 + 4/k)]^{1/2}\}^{1/2}$, then the m roots greater than $\eta_o = 0$ are given by

$$\eta_m = \begin{cases} [\pi^{-1} \tan^{-1}(D^-) + (m - 1)] \cdot F & \text{for } m = 1, 6, 11,\ldots \\ [\pi^{-1} \tan^{-1}(D^+) + (m - 1)] \cdot F & \text{for } m = 2, 7, 12,\ldots \\ [1 - \pi^{-1} \tan^{-1}(D^-) + (m - 1)] \cdot F & \text{for } m = 3, 8, 13,\ldots \\ [1 - \pi^{-1} \tan^{-1}(D^+) + (m - 1)] \cdot F & \text{for } m = 4, 9, 14,\ldots \\ m \cdot F & \text{for } m = 5, 10, 15,\ldots \end{cases}$$

The root $\eta_o = 0$ yields the first term, unity, in the brackets of Eqs. (14) and (15).

REFERENCES

1. P. Braunlich, J. Gasiot, P. J. Fillard, and M. Castagné, Appl. Phys. Lett. 39, 769 (1981).
2. J. Gasiot, P. Braunlich, and J. P. Fillard, J. Appl. Phys. 53, 5200 (1982).
3. P. Braunlich, S. C. Jones, A. Abtahi, M. deMurcia, and P. Kelly, Radiation Protection Dosimetry 6, 83 (1984).
4. P. Braunlich, W. Tetzlaff, J. Gasiot, and S. C. Jones, Proceedings of the International Beta Dosimetry Symposium, Washington, D.C., 293 (1984), NUREG/CP-0050.
5. A. Abtahi, P. Braunlich, and P. Kelly, J. Appl. Phys. 58, 1626 (1985).
6. W. Tetzlaff, P. Braunlich, and K. Swinth, Proceedings of the DOE Workshop on Beta Measurement, Albuquerque, NM, Jan. 23 - 24, 1986 (to be published).
7. P. Braunlich and W. Tetzlaff (Patent Pending), Serial No. 652, 829 Case No. US-5 (1985).
8. J. I. Frankel, B. Vick, and M. N. Ozisik, J. Appl. Phys. 58, 3340 (1985).
9. M. N. Ozisik, Heat Conduction (Wiley, New York, 1980).
10. H. H. Germand, The Rand Corp., RM-330 (1950).
11. J. I. Masters, J. Chem. Phys. 23, 1865 (1955).
12. Erie Scientific, Division of Syborn Corp., Portsmouth Industrial Park, Portsmouth, New Hampshire 03801.
13. S. W. S. McKeever, Nuc. Instrum. Methods 175, 19 (1980).
14. P. Kelly, A. Abtahi, and P. Braunlich (unpublished).

FIGURE CAPTIONS

Fig. 1. Schematic representation of a uniform circular beam profile impinging on the surface at z = 0 of a two layer system of total thickness L.

Fig. 2. (a) TL response curve measured with a 6.5 W CO_2 laser beam (ω = 0.1 5 cm for the uniform circular beam profile) by heating the phosphor coating on top of a glass substrate. The dashed curve is obtained with B = 7.3 K-cm^2/J, α = .0064 cm^2/s, using Eq. (14) of the text. The full curve is the fit obtained with B = 9.1 K-cm^2/J, the same α, and the Kirchhoff transformation.

(b) TL response when the laser beam impinges onto the side opposite to the phosphor coating. The dashed curve is the fit obtained with B = 5.8 K-cm^2/J at 6.5 W laser power, α = .0064 cm^2/s, using Eq. (15) of the text. The solid line is the fit obtained with B = 9.7 K-cm^2/J, the same α, and the Kirchhoff transformation.

Fig. 3. (a) TL response curves from Fig. 12 Ref. 5 recalculated using a 4.45 W CO_2 laser beam with a Gaussian intensity profile by heating the phosphor-coated side on a glass substrate. The families of curves are the fit obtained with B = 5.17 K-cm^2/J with the Kirchhoff transformation (solid lines) and B = 4.05 K-cm^2/J without the Kirchhoff transformation (dashed lines) using α = .0064 cm^2/s, the same as Fig. 2 for the following full widths at 1/e of the peak intensity of the laser beam 2ω (mm): 2.03, 1.83, 1.65, 1.45, 1.24 (curves from left to right, respectively).

(b) TL response curves from Fig. 13 Ref. 5 recomputed with a 4.18 W Gaussian laser beam by heating TL coating through the glass substrate. The dashed curves are obtained with B = 3.35 K-cm^2/J and the solid lines are curves obtained with B = 4.3 K-cm^2/J, using the Kirchhoff transformation and α = .0064 cm^2/s for the following measured beam widths 2ω (mm): 2.13, 1.994, 1.65 (curves from left to right, respectively).

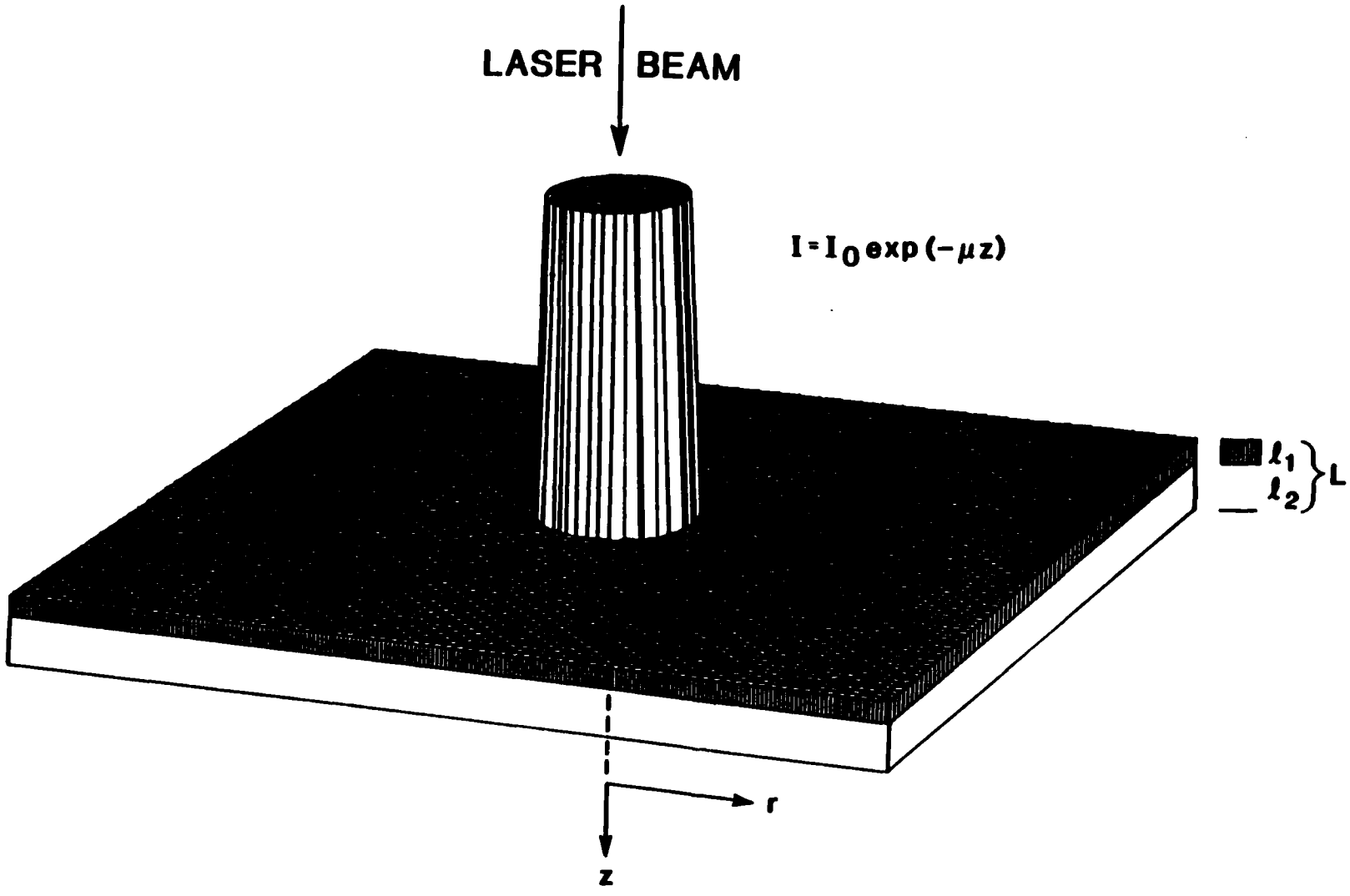
LASER BEAM
$I = I_0 \exp(-\mu z)$
l_1
l_2
L
r
z

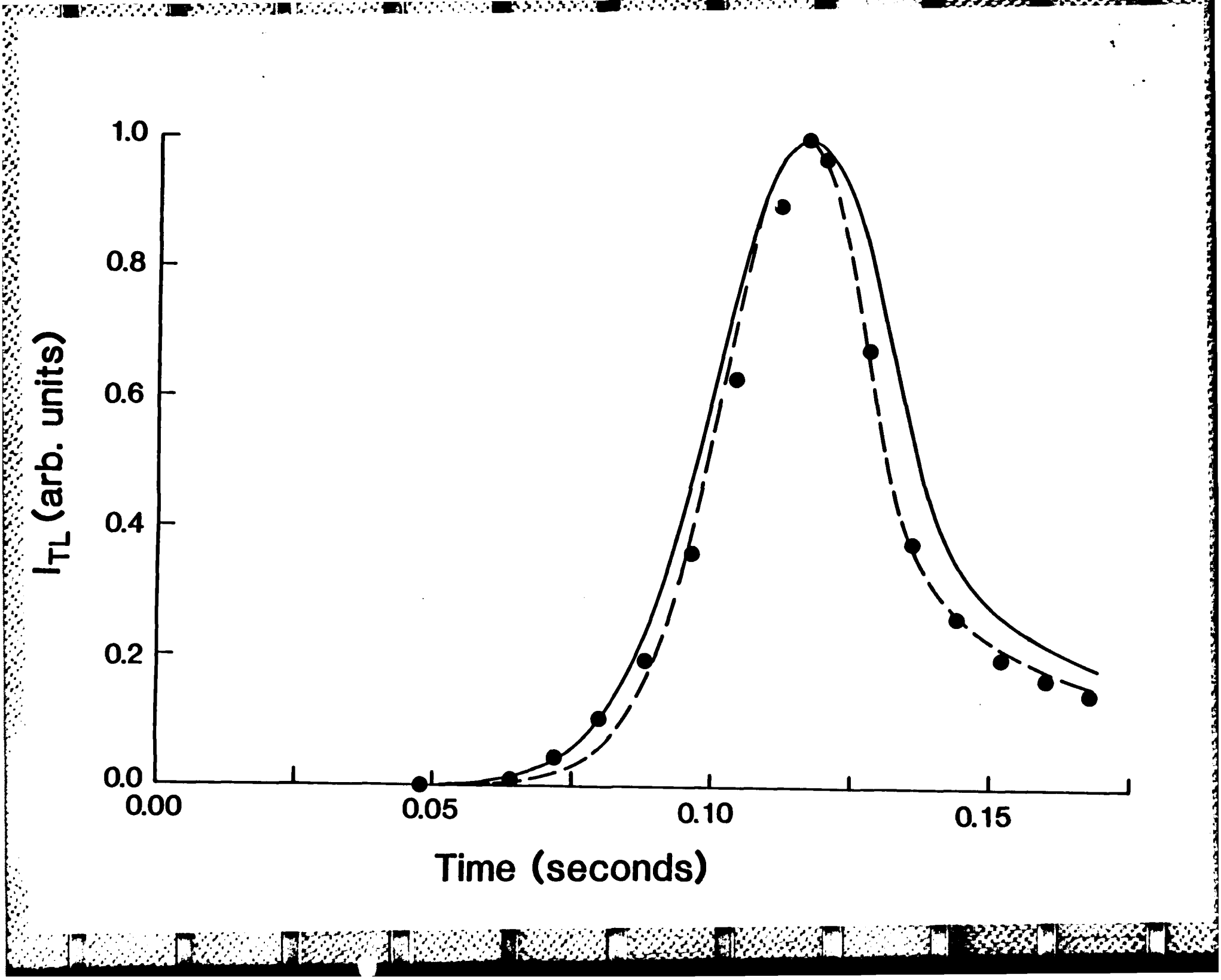
1.0
0.8
0.6
0.4
0.2
0.0
I_{TL} (arb. units)
0.00
0.05
0.10
0.15
Time (seconds)

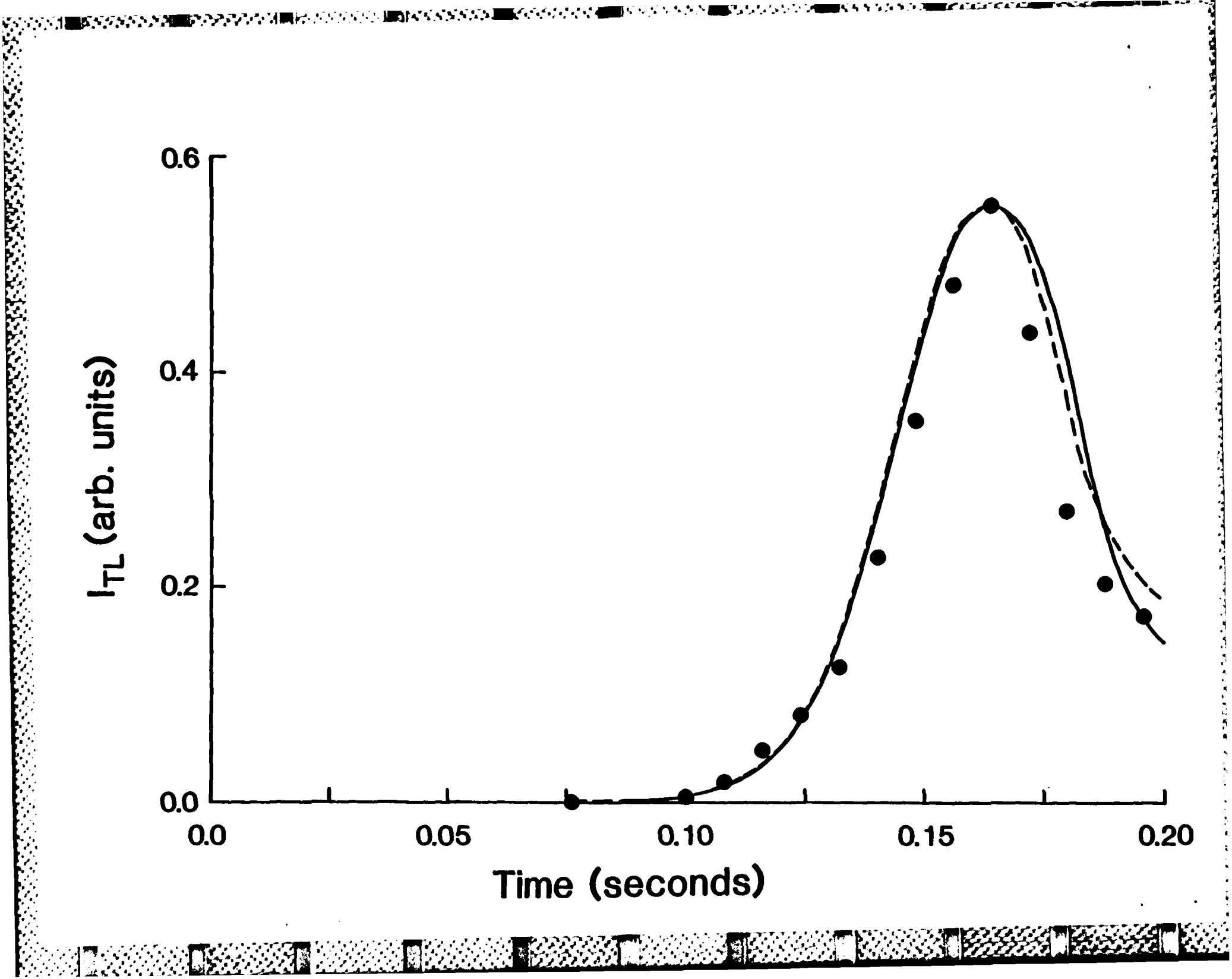
0.6
0.4
0.2
0.0
I_{TL} (arb. units)
0.0
0.05
0.10
0.15
0.20
Time (seconds)

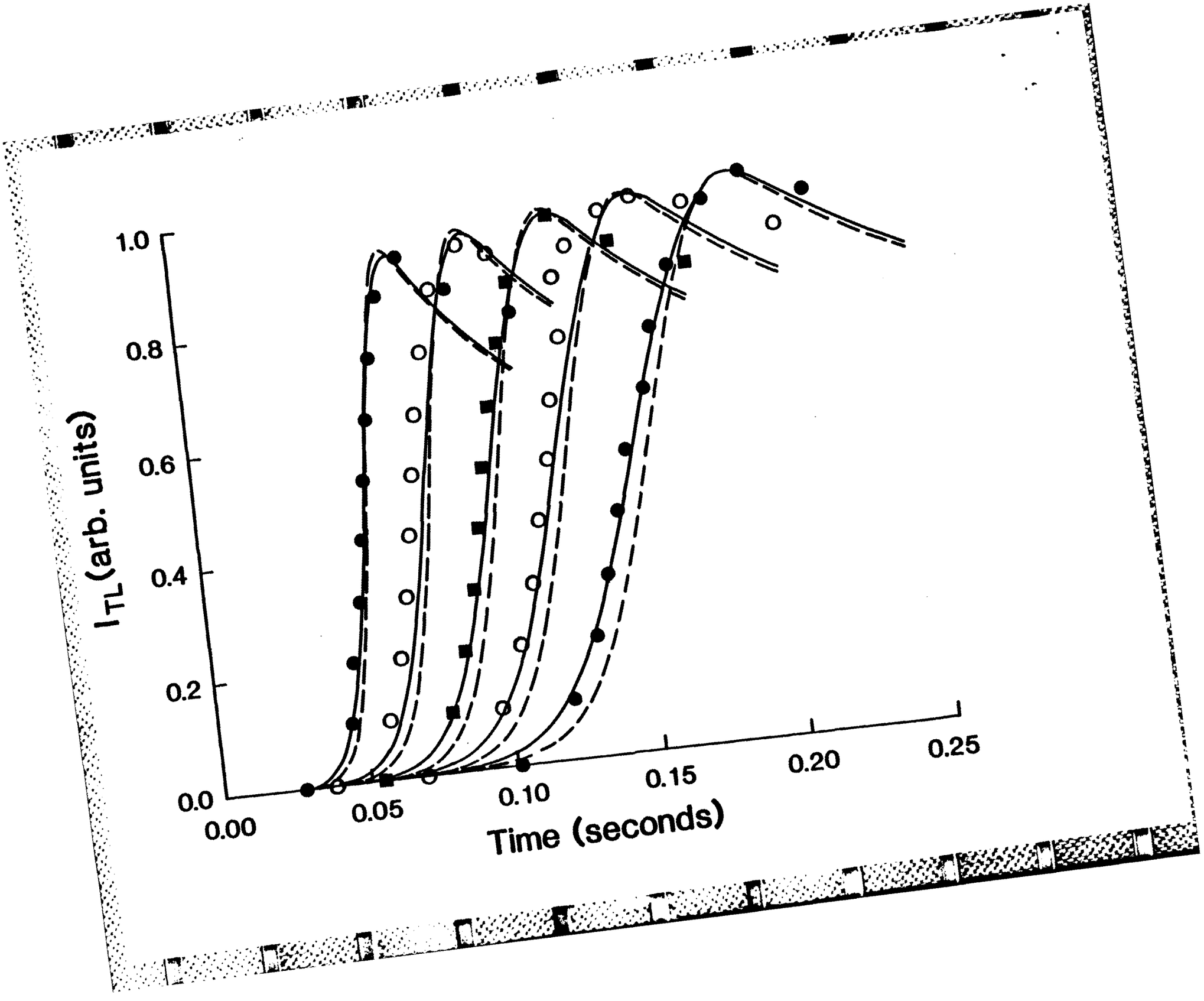
1.0
0.8
0.6
0.4
0.2
0.0
I_{TL} (arb. units)
0.00
0.05
0.10
0.15
0.20
0.25
Time (seconds)

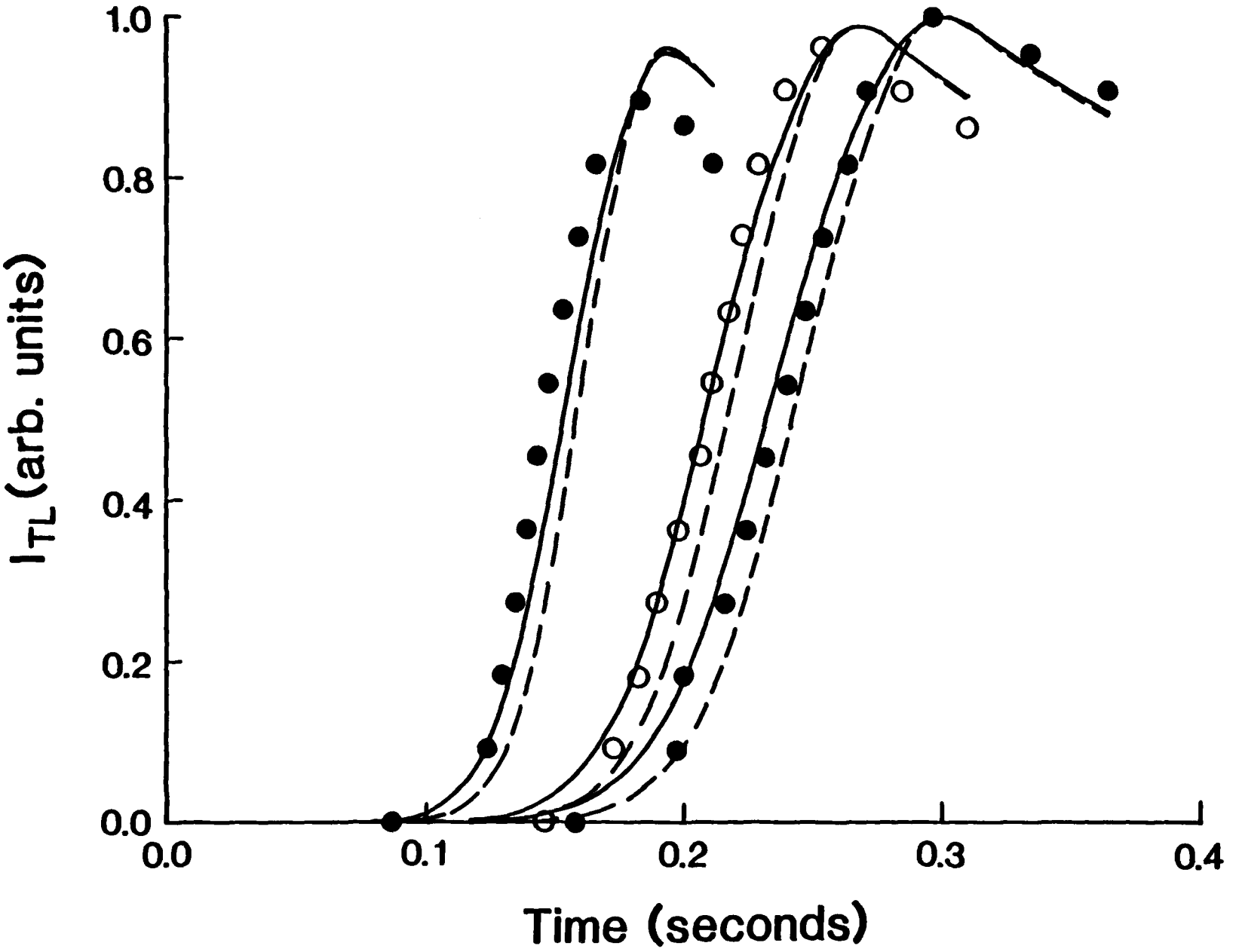
1.0
0.8
0.6
0.4
0.2
0.0
I_{TL} (arb. units)
0.0
0.1
0.2
0.3
0.4
Time (seconds)

LASER STIMULATED THERMOLUMINESCENCE II

by

Paul Kelly
Division of Microstructural Sciences
National Research Council
Ottawa, Canada K1A OR6

and

Abdollah Abtahi and Peter F. Braunlich
Department of Physics
Washington State University
Pullman, WA 99164-2814

ABSTRACT

The theory of heating a semi-infinite two-layer system with a localized CO_2 laser beam of uniform circular intensity profile is applied to configurations consisting of thin thermoluminescent LiF:Ti,Mg phosphor layers on borosilicate glass substrates. We study thermoluminescence because it serves as a convenient monitor for the temperature distribution and because of its importance in developing the laser heating technique for solid-state dosimetry. Experimental and calculated results are compared in an attempt to completely characterize the thermoluminescence response curves. The two-layer system is heated in two different modes: the laser beam impinges onto (a) the phosphor layer, and (b) the glass substrate. We investigate in detail changes in the thermoluminescence response due to different laser powers and variations in the optical and thermal properties of the samples.

I. INTRODUCTION

In a previous publication [1], henceforth referred to as I, computational methods were presented for the characterization of the thermoluminescence (TL) response obtained from thin semi-infinite thermoluminescent phosphor layers on transparent substrates upon exposure to localized Gaussian laser beams. These luminescence responses (the thermoluminescence intensity measured without spatial resolution) are not the familiar TL glow curves [2], but rather exhibit a complex shape with limited glow peak separation, which is the result of the extreme non-uniform laser beam profile and the resulting non-uniform temperature distribution in the sample. At any given time after onset of laser exposure, the lateral temperature distribution is nearly Gaussian as well, modified somewhat by thermal diffusion. The spatially resolved TL emission from the thin layer resembles such a Gaussian distribution up to times nearly 2.5 times longer than the appearance of the peak of the spatially unresolved TL response curve [3]. This curve typically exhibits a fast rise and a shallow peak, but never decays completely because of lateral heat diffusion [1]. The TL signal disappears only when the laser is turned off.

Laser heating of thin-layer thermoluminescent dosimeter configurations with focused Gaussian beams has been applied successfully to TL imaging [4] and to rapid measurement of dose distributions generated by exposure to beta rays behind attenuating filters of various thicknesses [5].

For accurate and sensitive personnel and environmental thermoluminescence dosimetry, heating with a laser beam of uniform intensity profile is, however, highly desirable. As we will demonstrate below, localized laser exposure of a semi-infinite phosphor layer on a substrate produces glow curves which are, except for a slowly decreasing tail at the high temperature side of the peak, nearly identical to the ones obtained with conventional uniform heating.

In this paper we describe a TL laser heating apparatus that features a circular beam of uniform intensity profile generated with a technique reported in Refs. 6 and 7. It was

employed to study the thermoluminescence response curves from thin-layer LiF:Ti,Mg dosimeters on glass substrates under a variety of experimental conditions. The motivation for this investigation was, however, not limited to the establishment of the operating conditions for efficient and economical laser heating in thermoluminescence dosimetry and imaging (the latter with greatly improved spatial resolution as compared to the non-uniform Gaussian beam). We also felt that the thermoluminescence emission from a thin layer on a substrate is a very convenient monitor for the time-evolution of the temperature distribution established in the two-layer system during localized heating with a laser beam of uniform intensity profile. The general theory of the heat transfer from such a beam to a semi-infinite two-layer system and the subsequent temperature diffusion was presented previously [3,8]. In the following we will first briefly review the basic aspects of this theory, describe the experimental facility in some detail, and finally present experimental and computation results.

II. COMPUTATIONAL APPROACH

In applying the theory of Ref. 8 to a special system that consists of a thin thermoluminescent phosphor layer on a strongly absorbing substrate, a number of approximations can be made which greatly reduce the computational effort required for simulating thermoluminescence response curves measured under various different experimental conditions. The justification for these assumptions is discussed in detail in Section IV. Here we only briefly review the important features of the simplified theory.

Assume a system that consists of a thermoluminescent phosphor layer on a glass substrate in perfect thermal contact. Each layer is characterized by its absorption coefficient for the laser photons, μ_i, thermal conductivity, k_i, and thickness l_i. The index i = 1,2 denotes the respective layer and the total thickness is $L = l_1 + l_2$. In contrast to the general theory, we assume for the special case of a thin phosphor layer on a thicker glass slide that the thermal diffusivity, α_i, is temperature independent and identical for both layers. The

laser beam has a fixed diameter and a uniform circular intensity profile which is cylindrically symmetric around the beam axis. It enters the two-layer system perpendicular to the x-y plane either from the side of the phosphor layer or the glass substrate. The absorptance (absorbed fraction of the incident laser power) is of course different in both cases, and so is the co-called prefactor B in the expression for the temperature rise (Eq. 1 below). The thermal diffusion equation and the appropriate boundary and initial conditions for this problem are stated in Ref. 8.

Accounting for first-order reflection losses on the surface of incidence and at the layer interface, the spatio-temporal distribution of the temperature rise for the two layers is given by [8]

$$\Delta T_i(r,z,t) = (BP^*/\omega^2) \int_0^t d\tau\, Q(t-\tau)\{1 + [(1 - R_1)/\pi B] \sum_{m=1}^{\infty} \exp(-\mu_1 l_1)[\exp(-\mu_1 l_1)\cos(\eta_m l_1) + (\eta_m/\mu_1)\sin(\eta_m l_1)]/ [N_m(1 + \eta_m^2/\mu_1^2)\cos(\eta_m/\mu_1 l_1)] + (1 - R_2) \exp(-\mu_1 l_1)[\cos(\eta_m l_2) + (\eta_m/\mu_2)\sin(\eta_m l_2) - \exp(-\mu_2 l_2]/ [N_m(1 + \eta_m^2/\mu_2^2)\cos(\eta_m l_2)]\} x_i(z)\exp[-\alpha\eta_m^2(t-\tau)] \quad (1)$$

where P^* is the total laser power (not the power density) incident on the front surface, R the reflectivity layer i, ω the radius of the uniform circular beam. We further have $B = (1 - R_1)[1 - (1 - R_2)\exp(-\mu_1 l_1 - \mu_2 l_2) - R_2 \exp(-\mu_1 l_1)]/\pi N_o$, $N_o = (1/\alpha) \sum_{i=1}^{2} k_i l_i$, and $N_m = (1/2\pi) \sum_{i=1}^{2} k_i l_i [1 + \sin 2\theta_i/2\theta_i] \cos^2\theta_i$ with $\theta_i = .\eta_m l_i$, and $Q(t) = P(\omega)/\sqrt{2\alpha t}$, $r/\sqrt{2\alpha t}$). $P(\omega,r) = \int_0 \omega' d\omega' I_o(\omega',r) \exp[-(\omega'^2 + r^2)/2]$ is called the circular coverage function. The parameters η_m (m = 1,2, ...) are the roots of the following transcendental equation (see Appendix A)

$$k_1 \tan \eta_m l_1 + k_2 \tan \eta_m l_2 = 0, \quad (2)$$

which arises from the boundary conditions.

An additional simplification of Eq. (1) is possible. It stems from the fact that the material of interest in our studies, LiF, is not a strong absorber for the 10.6 μm photons of the laser heating beam ($\mu = 40\ cm^{-1}$). In contrast to this, the absorption coefficient of the glass substrate is very high. Consequently, the laser deposits the energy directly into the interface between the layers if it impinges on the phosphor side of the two-layer system (Case 1 below). On the other hand, it is possible to direct the laser beam onto the glass side of the system where it is completely absorbed at the surface (Case 2). Thus the active thermoluminescent layer can be located between $z = 0$ and $z = l_1$ (Case 1) or between $z = l_1$ to $z = L$. The appropriate expressions for the temperature rise in these cases are readily obtained from Eq. (1):

Case 1: thermoluminescent layer on top of the glass substrate

$(\mu_1 l_1 << 1)$

$$\Delta T_1(r,z,t) = (BP^*/\omega^2) \int_0^t d\tau\, Q(r,t-\tau)\{1 + N_0 \sum_{m=1}^{\infty} \cos(\eta_m z) \exp[-\alpha\eta_m^2 (t-\tau)]/[N_m(1 + \eta_m^2/\mu_2^2) \cos(\eta_m l_1)]\} \quad (3)$$

Case 2: thermoluminescent layer at the bottom of the glass substrate

$(\mu_2 l_2 << 1)$

$$\Delta T_2(r,z,t) = (BP^*/\omega^2) \int_0^t d\tau\, Q(r,t-\tau)\{1 + N_0 \sum_{m=1}^{\infty} \cos(\eta_m (L-z)) \exp[-\alpha\eta_m^2 (t-\tau)]/[N_m(1 + \eta_m^2/\mu_1^2) \cos(\eta_m l_1) \cos(\eta_m l_2)]\} \quad (4)$$

The actual computer calculations of the thermoluminescence response are based on the well-known first-order electron kinetics of the LiF:Ti,Mg phosphor (TLD-100, Harshaw/Filtrol) and require knowledge of the heating rates in each volume element $2\pi r dr dz$. These are:

Case 1: $(\mu_1 l_1 << 1)$

$$\partial T_1(r,z,t)/\partial t = (BP^*/\omega^2)\, d\tau\, Q(r,t)\{1 + N_o \sum_{m=1}^{\infty} \cos(\eta_m z)$$

$$\exp(-\alpha\eta_m{}^2\psi[N_m(1 + \eta_m{}^2/\mu_2{}^2)\cos(\eta_m l_1)]\} \qquad (5)$$

Case 2: $(\mu_2 l_2 << 1)$

$$\partial T_2(r,z,t)/\partial t = (BP^*/\omega^2)\, d\tau\, Q(r,t)\{1 + N_o \sum_{m=1}^{\infty} \cos(\eta_m (L-z))$$

$$\exp(-\alpha\eta_m{}^2\psi[N_m(1 + \eta_m{}^2/\mu_1{}^2)\cos(\eta_m l_1)\cos(\eta_m l_2)]\} \qquad (6)$$

The luminescence glow peaks of the LiF:Mg,Ti considered are commonly called peaks 3, 4, and 5. They are well described by first-order kinetics with attempt-scape-frequency of $4 \times 10^{13}\ s^{-1}$, $7.3 \times 10^{15}\ s^{-1}$, and $4 \times 10^{21}\ s^{-1}$ and trap depth of 1.23 eV, 1.54 eV, and 2.17 eV, respectively [9].

The sum of the relative peak heights [9] of the LiF:Ti,Mg glow curve is used as a measure for the total trapped electron population, and the relative population of each of the three electron trap levels is taken to be proportional to its corresponding peak height with the correction of luminescence efficiency at different heating rates [10]. TL peaks that occur at temperatures lower than those of peaks 3 to 5 are eliminated by a preannealing for 10 minutes at 100°C.

The three first-order electron-kinetic differential equations for peaks 3 to 5 [9] are solved with these heating rates by the Runge-Kutta method for each volume element $2\pi r dr l_1$ (for case 1) or $2\pi r dr l_2$ (for case 2). Because the phosphor layer is very thin, integration over the phosphor layer thickness is omitted (see Fig. 11 below). In Section IV this assumption will be justified by comparison of measured and calculated

thermoluminescence response curves. The numerical integration is sufficiently precise with step sizes $\Delta r = 1.25\omega/50$, and $\Delta t = 10^{-3}\, t_p$, where t_p is the total time of laser exposure, except for the first millisecond during which $\Delta t = 10^{-6}\, t_p$.

III. EXPERIMENTAL SETUP

The experimental arrangement is schematically shown in Fig. 1. A temperature-stabilized radio frequency-excited cw CO_2 laser (Directed Energy Inc. model L35-PS) emits a beam whose intensity profile has an annular ("halo") cross section of 1 cm diameter. The 10.6 μm photon beam is linearly polarized. The maximum output power is 40 Watts. For closed-loop control of the laser beam, the RF power supply is modified for pulse-width modulation at 34 kHz with a variable duty cycle that determines the laser output power.

The beam is guided to a focusing module by two parallel gold-coated copper mirrors. It enters the light-tight optical chamber through an AR-coated Ge window. The focusing module deflects the beam down onto the entrance of the so-called beam equalizer channel [6], which produces a uniform square beam of 3 x 3 mm^2 area. To simplify the theory and the numerical calculation, the square profile of the output beam is converted to a circular one with the aid of a 2.95 mm diameter aperture at the channel exit. The sample holder is placed in close proximity to it so that, at the top of the sample, the beam has diverged only to about 3 mm diameter.

A gold-plated electro-mechanical shutter, placed in front of the channel, controls the exposure time of the sample to the laser beam. When it is closed, the laser beam is reflected into a beam dump.

To provide a signal for closed-loop control of the laser power, an anti-reflection coated ZnSe window reflects a small fixed portion (3 to 5 percent) of the laser beam to a piezoelectric detector (Barnes Engineering Inc. model 350-5 PZT). A beam chopping wheel operated at 33.5 cycles/s by a dc motor is placed in front of the detector in order to

prevent saturation. The output of the detector is fed to the electronic control unit, providing an updated laser power measurement every 9.3 ms. In this way, the laser output power is kept constant within 2-3 percent.

A TL sample on a 25 x 25 mm^2 substrate can be placed in a sample holder at a distance of 40-50 μm from the end of the channel. A specific area of the sample, selected by a pair of coupled translation stages, can be heated by the laser beam. In this way up to 35 spots on a continuous TL sample can be heated separately. Typical exposure times range from 100 ms to 10 seconds. The translation stages are connected to two motor driven actuators which are controlled by a motor drive system with a positioning accuracy of up to 0.1 μm.

The emitted light from a TL sample is transmitted by a light guide, through a shutter, and a protective glass window to a photomultiplier tube (EMI type 9924B). The shutter and glass plate prevent the PMT from accidental exposures to visible light or the unimpeded laser power, respectively. The light guide channel is 12.5 mm diameter buffed stainless steel tube. To maximize the collection efficiency of the emitted thermo-luminescence, one end of it is placed in close proximity to the heated area on the sample. The current signal of the PMT is measured, processed, stored, and displayed with the aid of a transient digitizer.

The electronic control unit of the apparatus performs such functions as timing, controlling, and protecting the system.

When a TLD reader heating cycle is activated, the following sequence is performed by the control electronic:

The laser is turned on and its output power is measured and adjusted until the laser is stabilized at the desired power level. This process is normally accomplished in 100 to 300 ms; however, it may require a longer time if the laser happens to be in an undesirable operating condition. During this time, the shutter remains closed and the sample is not exposed to the beam. After the desired laser power is obtained, the shutter is open for a set

desired heating time. At the end of the heating cycle, the shutter will close and the laser is turned off.

IV. RESULTS AND DISCUSSION

As in I, we have chosen LiF:Ti,Mg (TLD-100 supplied by Harshaw/Filtrol) as the thermoluminescent material to serve as a monitor of the temperature evolution when the two-layer system is exposed to the laser beam. All systems we studied consisted of a 35-40 μm thick fine-grain phosphor layer in a high-temperature binder on 150 μm thick 25 x 25 mm^2 borosilicate glass microscope cover slides. After exposure to ^{60}Co gamma rays (for the purpose of filling the traps) and a subsequent 10 minute pre-anneal treatment to eliminate low-temperature glow peaks [1], the center of these samples was heated with a stable and uniform 3 ± 0.07 mm diameter CO_2 laser beam whose power could be varied between 13.5 Watts and 2.44 Watts. The laser exposure was done in two different modes, the laser beam either striking the front (phosphor layer) or the back (substrate,. Naturally, the so-called prefactor B (see Section II), which is essentially a measure of the absorptance, is different for these two modes of laser exposure. With the method described in I its value was determined to be $B = 10.7 \pm 25\%$ K-cm^2/J for the phosphor layer surface and $B = 6.3 \pm 20\%$ K-cm^2/J for the glass substrate surface (note that B is defined slightly differently as compared to the definition used in I; here it is divided by the laser power P). The electron-kinetic data of the traps that we exploited in our experiments are given in Section II.

In an initial set of tests we established the validity of a number of assumptions and approximations that can be made to reduce the computational effort required for the comparison of experiments and the theory, without severely impacting the results.

The first of these approximations concerns the method of the Kirchhoff transformation described in I. It permits one to account for the temperature dependence of the thermal conductivity of the glass substrate, which we approximated as $k_2 = 0.00942$

$(1 + 0.00222\ \Delta T_2)$ W/Kcm, based on data given by the glass manufacturer [11]. In Fig. 2 the TL response curve is shown that was measured by exposing the glass layer (Case 2: heating from the back of the sample) to a 9.75 W laser beam together with calculations based on Eqs. (4) and (6) and in conjunction with the simplifying assumptions discussed below. The Kirchhoff transformation yielded the dashed line, and the solid line was obtained assuming constant $k_2 = 0.00942$ W/Kcm. In view of the rather good agreement between theory and experiment that is achieved without accounting for the temperautre dependence of k, we decided to disregard the Kirchhoff transformation for all cases described in this paper. We have checked this with a number of different experimental situations and found it was always justified in applications of the theory of Ref. 8 to thin two-layer thermoluminescence dosimeter configurations.

A second simplification concerns the thermal diffusivity of the two layers. Because the phosphor layer is very thin and does not strongly absorb the laser photons, but the glass substrate is a very strong absorber, the laser energy is deposited in the interface, when the system is heated from the front (Case 1). The phosphor layer is indirectly heated by diffusion, which is rather rapid in z-direction, because its so-called thermal response time or diffusion time [12], $t_0 = \ell^2/\alpha$, is estimated to be about 1 ms. This is much shorter than the time required to measurably change the thermoluminescence intensity even at the highest laser power densities that appear practical for this type of heating in thermo-luminescence dosimetry [7]. Assuming the thermal diffusivity of the phosphor layer is not significantly greater than that of the glass substrate, heat transport by lateral thermal diffusion occurs mainly in the thicker of the two layers with essentially instantaneous diffusion in z-direction through the thin layer. This is of course also true for Case 2 (laser heating from the back). Therefore, we are justified to assume the thermal diffusivity of both layers to be equal, its value being that of glass [3]. Actually, there is a reason to assume that the thermal diffusivity of the phosphor layer is rather small, perhaps even smaller than that of glass. This layer is a loosely packed matrix of small grains in a poor

heat conductor (Dow Corning 805 silicone). Since the thermal diffusivity, α, for glass is slightly temperature dependent (varying from 0.0052 cm^2/s at 0°C to 0.0057°C at 100°C, but it is unknown for higher temperatures), and since we did not choose to account for this, we had the problem of selecting a proper "temperature-averaged" value that provided a good approximation for all calculations presented below. We established that value as α = 0.0064 cm^2/s by the best fit of families of TL response curves measured for front and back exposure with several different laser powers (Fig. 3 is an example). This high value appears justified when one considers the fact that the TL glow peaks we selected as "temperature indicators" for our experiments reach their maximum emission intensity at about 250°C [9]. Consequently, the major portion of the thermoluminescence emission and thus the range of "temperature monitoring" occurs well above 100°C. It should be pointed out that the decay of glow curve is very sensitive to the value of α as shown in Fig. 4.

Yet another simplification of the computational procedure is possible because the TL phosphor layer is so thin and diffusion across it is relatively rapid. Instead of calculating the transient TL emission from infinitesimally thin layers δz and integrating over z from $z = 0$ to $z = l_1$, it suffices to calculate the TL emission either from the surface layer at $z = 0$ or from the interface layer at $z = l_1$. The total instantaneous emission is then obtained simply by multiplying with the thickness, l_1, of the active layer. In each situation good agreement results between theory and measurement. This is demonstrated in Fig. 5, where the case of Fig. 2 is recalculated for different values of z. Henceforth, we arbitrarily choose to take the computed TL emission from the interface at $z = l_1$ to represent the emission from the entire layer.

We repeat, these simplifications were introduced solely to reduce the computational effort, because the so executed calculations yield results that agree with measurements within the experimental errors. They are not strictly required as the more exact calculations pose no problems in principle.

Even though we have not yet measured in detail spatially resolved thermoluminescent responses from a TL phosphor layer on a glass slide that is heated with a localized uniform laser beam, we present here some initial computational results as they help to visualize the relation between the spatio-temporal temperature distribution and the corresponding thermoluminescent response. Figure 6(a) shows the temperature distribution in the phosphor-glass interface at t = 4 ms after onset of exposure of the phosphor layer to a uniform 3 mm diameter laser beam of 6.5 Watt power. At $t = t^* = 115$ ms (here t^* is the time of TL peak occurrence), the distribution is considerably different due to heat diffusion (Fig. 6b). Interestingly, the lateral distributions of the TL emission appears to retain the basically cylindrical shape up to t^*; it simply broadens with heating time. This is of course a result of the initial rise of a glow curve which is proportional to $\exp(-E/kT)$ (E is the thermal activation energy). Immediately after t^*, the TL intensity decreases in the central and hottest part of the exposed area, and where it has decreased essentially to zero at $t = 1.5\ t^*$, shown in Figs. 7(a)-7(c). For times $t > t^*$, the TL emission originates only from those areas of the phosphor layer that are not directly exposed to the laser beam, but are heated by lateral diffusion.

For applications of laser heating in thermoluminescence dosimetry it is of interest to investigate the temperature rise of the exposed phosphor layer. Optimum operating conditions are commonly believed to include heating a thermoluminescent dosimeter with a constant heating rate; i.e, a temperature rise linear in time [13]. Figure 8 shows computed temperature rise curves for the same sample and experimental conditions discussed above. In agreement with calculations by Sparks [12], the temperature in the center of the exposed spot rises first nonlinearly for a few ms and is linear thereafter. The heating rate is proportional to the laser power. The numerical calculations indicate further, that the heating rate is very nearly the same for an area centered around the laser beam axis up to a radius $0.5\ \omega$ for heating times well past the peak of the TL glow curve (compare with Figs. 4-7). This is of considerable practical importance as it demonstrates by the usefulness of laser

heating not only for dosimetry [3, 14, 15], but also in a number of special areas which exploit thermoluminescence; e.g., dating of archaeological artifacts and art authentication [16]. Very precise linear and reproducible heating is possible of minute fine-grain samples that are attached with a suitable binder to a substrate in the center of the uniform laser heating beam. We have successfully heated single <100 μm diameter grains of natural quartz and obtained strong TL signals without previous additional radiation exposures [17]. The reproducibility and accuracy of this heating technique depends, of course, on the stability and reproducibility of the laser beam. As mentioned in Section III, it is possible to control the laser power to within less than 3 percent.

One of the goals of our investigations was to establish the validity of the general laser heating theory presented in Ref. 8. An assessment of the achievable accuracy of the thermcluminescence temperature monitoring method was therefore essential. Experimental errors arise from the uncertainty in laser beam parameters, the phosphor layer uniformity, and the reproducibility with which the two-layer samples can be produced. With a stable laser power, only the beam radius, w, remained as a critical parameter. Calculations indicated that it very sensitively influences the TL glow curves. Changing ω by only ±1 percent yields shifts (Fig. 9) that otherwise are produced only by variation of the produced layer thicknesses (see below). For this reason the laser-heated thermoluminescence apparatus described in Section III was constructed with a fixed rather than a variable laser beam radius, and, therefore no experiments were performed to date with a heating beam of constant power but variable diameter.

Variations in the thickness, l_1, of the phosphor layer cause the TL response curves to shift and change in intensity. This is demonstrated in Figs. 10 and 11, which show a number of curves that were measured (Fig. 10) and calculated (Fig. 11) with different values of l_1. Figure 10 indicates the rather limited reproducibility of the spreading method used to fabricate the samples. Despite considerable effort, which involved the construction of a special layer spreading machine and careful control of the phosphor-binder mixture,

this performance could not be improved beyond the one reported here, and more work on layer fabrication techniques is needed. However, the layer uniformity achieved was sufficient for a study of the TL response of a number of nominally identical samples as a function of laser power. Typical measured and computed glow curves resulting from this study are shown in Fig. 12 (Case 1: the laser heating beam impinges onto the TL layer). For a best fit, the parameter B had to be adjusted slightly. Note that the variation in B is within the accuracy of the experimental method we used to determine it [1]. It was necessary to also account for the fact that the overall luminescent yield decreases with increasing heating rate for otherwise idential experimental conditions. Detailed measurement of the dependence of the yield on the heating rate will be presented in a forthcoming publication [10].

V. CONCLUDING REMARKS

We have compared experimental and computed thermoluminescence response curves obtained from two-layer configurations by localized heating with a 3 mm diameter CO_2 laser beam of uniform circular intensity profile of power up to 13 Watts. The results confirm the theory of Ref. 8 and show that thin-layer thermoluminescence dosimeters can be heated with heating rates up to 5500°C/s.

It is of particular importance that the thermoluminescence glow curves measured under these experimental conditions have the familiar shape obtained with conventional contact heating.

REFERENCES

1. A. Abtahi, P. Braunlich, and P. Kelly, J. Appl. Phys. 58, 1626 (1985).
2. P. Braunlich, ed., Thermally Stimulated Relaxation in Solids (Springer, Heidelberg, 1979).
3. A. Abtahi, Ph.D. dissertation, Washington State University, 1986.
4. Y. Yasuno, H. Tsutsui, O. Yamamoto, and T. Yamashita, Japan. J. Appl. Phys. 21, 967 (1982).
5. P. Braunlich, et al., Proceedings of the International Beta Dosimetry Symposium, Washington, D.C. (1983), U.S. Nuclear Regulatory Commission Publication No. NUREG/CP-00500, p. 293.
6. P. Braunlich and W. Tetzlaff, Patent Pending, Serial No. 652,829 Case No. US-5 (1985).
7. P. Braunlich and W. Tetzlaff, submitted for presentation at the 8th International Conference on Solid State Dosimetry, Oxford, U.K., August 26-29, 1986.
8. A. Abtahi, P. Braunlich, and P. Kelly (unpublished), 1986.
9. S. W. S. McKeever, Nuc. Instrum. Methods 175, 19 (1980).
10. A. Abtahi, P. Braunlich, and P. Kelly, submitted for presentation at the 8th International Conference on Solid State Dosimetry, Oxford, U.K., August 26-29, 1986.
11. Erie Scientific, Division of Syborn Corp., Portsmouth Industrial Park, Portsmouth, New Hampshire 03801.
12. M. Sparks, J. Appl. Phys. 47, 837 (1976).
13. M. Oberhofer and A. Scharmann, ed., Applied Thermoluminescence Dosimetry (Adam Hilger, Bristol, 1981).
14. W. Tetzlaff, P. Braunlich, and K. Swinth, Proceedings of the DOE Workshop on Beta Measurement, Albuquerque, 1986 (to be published).

15. P. Kelly, A. Abtahi, and P. Braunlich, submitted for presentation at the 8th International Conference on Solid State Dosimetry, Oxford, U.K., August 26-29, 1986.

16. M. J. Aitkin, Physics and Archaeology, 2nd ed. (Clarendon, Oxford, 1974).

17. J. Gasiot, et al. (unpublished).

APPENDIX A

In this work we have a poorly absorbing phosphor coating $l_1 = 0.2L$ on a highly absorbing glass slide, $l_2 = 0.8L$ where the total thickness $L = 0.01875$ cm. In this case m distinct roots η_m can be obtained from the transcendental equation $k_1 \tan\theta + k_2 \tan 4\theta = 0$ with $\theta = 0.2\eta_m L$. With $F = 5\pi/L$, $h = 3+2/k$, $k = k_1/k_2$, $D^+ = \{h + [h^2 - (1 + 4/k)]^{1/2}\}^{1/2}$ and $D^- = \{h - [h + (1 + 4/k)]^{1/2}\}^{1/2}$, then the m roots greater than $\eta_o = 0$ are given by

$$\eta_m = \begin{cases} [\pi^{-1} \tan^{-1}(D^-) + (m - 1)] \cdot F & \text{for } m = 1, 6, 11,\ldots \\ [\pi^{-1} \tan^{-1}(D^+) + (m - 1)] \cdot F & \text{for } m = 2, 7, 12,\ldots \\ [1 - \pi^{-1} \tan^{-1}(D^-) + (m - 1)] \cdot F & \text{for } m = 3, 8, 13,\ldots \\ [1 - \pi^{-1} \tan^{-1}(D^+) + (m - 1)] \cdot F & \text{for } m = 4, 9, 14,\ldots \\ m \cdot F & \text{for } m = 5, 10, 15,\ldots \end{cases}$$

The root $\eta_o = 0$ yields the first term, unity, in the brackets of Eq. (1).

FIGURE CAPTIONS

Fig. 1. Schematic experimental arrangement of the laser thermoluminescence apparatus.

Fig. 2. Thermoluminescence response curves measured and calculated with a uniform laser beam of 3 mm diameter and 9.75 Watts power heating a 37.5 μm thick TL layer through a 0.15 mm thick borosilicate glass substrate (the laser beam impinges onto the glass substrate). The solid line is computed with a constant thermal conductivity of the glass $k = 0.00942$ W/Kcm and the dashed line with the method of the Kirchhoff transformation, which takes into account the temperature dependence of k [1]. With the thermal diffusivity $\alpha = 0.0064$ cm^2/s (see Fig. 3), the parameter B was determined to be 6.4 Kcm^2/J by the best fit to the measured curve. This value agrees well with the experimentally determined one: $B = 5.7 \pm 20\%$ Kcm^2/L (see Ref. 1). Prior to the measurement of the TL response curve, the sample was exposed to gamma rays from a ^{60}Co source and pre-annealed for 10 minutes at 100°C.

Fig. 3. Thermoluminescence response curves measured by heating with laser beams of fixed 3 mm diameter but different powers impinging onto the glass side of the two-layer system. The sample is a 37.5 μm thick LiF:Ti,Mg on a 0.15 mm thick borosilicate glass substrate. The family of curves, calculated from Eqs. (4) and (6), yields the value $\alpha = 0.0064$ cm^2/s for the thermal diffusivity via best fit with the measurements. The calculations were performed with $k_1 = 0.00942$ W/Kcm that is characteristic for the system and the following laser powers and B parameters:

P* =	13	Watts	B = 6.3	Kcm^2/J
	9.75	Watts	6.4	Kcm^2/J
	6.5	Watts	6.0	Kcm^2/J
	4.875	Watts	6.3	Kcm^2/J

Peaks 1 and 2 of LiF:Ti,Mg (TLD-100, Harshaw/Filtrol) were removed by 10 minutes preannealing at 100°C [9].

Fig. 4. Computed thermoluminescence response curves of the sample from Fig. 3 for various thermal diffusivities, α. The best fit with the measured curve is obtained with $\alpha = 0.0064$ cm^2/s and the prefactor B = 6.0 Kcm^2/J (dotted curve). The effect of different thermal diffusivities is demonstrated by the solid ($\alpha = 0.005$ cm^2/s) and the dashed ($\alpha = 0.0078$ cm^2/s) lines. Laser power: $P^* = 6.5$ Watts.

Fig. 5. Thermoluminescence response curves obtained for the sample and experimental conditions as in Fig. 4, computed for different depths, z, of the active layer. The dashed line represents the normalized thermoluminescence emission from a thin sheet at z = L (the surface of the TL layer), and the solid line that at $z = l_1$ (the interface of the TL layer and the glass substrate). We have adjusted the parameter B so that the occurrence of the peak emission is the same as that of the measured curve: B = 6 Kcm^2/J (dashed line) and B = 5.2 Kcm^2/K (solid line). The calculations demonstrate that for thin TL layers the z dependence of the TL response is small.

Fig. 6. Computer simulations for the normalized spatial temperature distributions T(r,z,t) calculated for exposure of a phosphor layer on a glass substrate to a 6.5 W-laser heating beam with a uniform circular intensity profile, $2\omega = 3$ mm. The calculations are performed with B = 7.55 Kcm^2/J, $\alpha = 0.0064$ cm^2/s and a total thickness L = 0.1875 mm for various times after onset of laser exposure: a) t = 4 ms and b) $t = t^* = 115$ ms (the peak intensity of the thermoluminescence response occurs at t).

Fig. 7. The normalized spatial distributions of the thermoluminescence response calculated for the sample from Fig. 6 at various times with respect to the time, T*, of the TL peak intensity occurrence, t which are: a) $t = 1/2\ t^*$, b) $t = t^*$, and c) $t = 1.5\ t^*$.

Fig. 8. Computed time evolution of the temperature of the sample and experimental conditions as in Fig. 6 at various distances, r, from the laser beam axis: r = 0, $\omega/4$, $\omega/2$, ω, 1.125 ω (from top to bottom). ($w = 0.15$ cm is the radius of the laser beam.)

Fig. 9. Calculated thermoluminescence response curves of the sample from Fig. 3 for small variation in the radius of the laser beam. The computations are performed with $P^* = 6.5$ Watts and the following beam radii w (from left to right): 0.1485, 0.15, and 0.1515 cm.

Fig. 10. A set of thermoluminescence response curves measured with a 37. 5 μm thick TL layer on 0.15 mm thick borosilicate glass substrate for fixed laser beam radius w = 0.15 cm and various laser powers P^*. The laser beam impinges on the phosphor side of the sample. To check the reproducibility of the measurements, several thermoluminescence responses from different sites on the sample were measured for otherwise identical conditions with the following laser powers (in Watts): 1) 13, 2) 9.75, 3) 6.5, 4) 4.875, 5) 3.25, and 6) 2.44.

Fig. 11. Computed normalized thermoluminescence response curves for various total thicknesses, L, but fixed ratio $l_1/l_2 = 1/4$. Otherwise the sample is identical to that of Gi. 3. The calculations were performed with a laser power of 6.5 Watts and the following thicknesses (from left to right): 0.094, 0.178, 0.1875, 0.197, and 0.375 mm.

Fig. 12. Measured and computed thermoluminescence response curves of the sample from Fig. 10, and the same experimental conditions. The dashed curves are computed from Eqs. (3) and (5) and the first-order electron kinetics parameters determined by McKeever [9] for peaks 3-5 of LiF:Ti,Mg and by taking into account the measured decrease in luminous efficiencies with increasing heating rates. Again, peak 2 was removed by a 10 minute preannealing at 100°C. With the thermal diffusivity $\alpha = 0.0064$ cm^2/s and a laser beam radius of $w = 0.15$ cm, the parameter B was determined for each curve by the best fit. The results are calculated with the following luminescence efficiencies, η (in % of the value obtained for the smallest heating rate): 81.8, 81.9, 85.5, 89.6, 95.7, and 100

(from left to right). The parameters B (Kcm^2/J) are: 8.53, 7.93, 7.55, 7.30, 7.17, and 7.00 (from left to right).

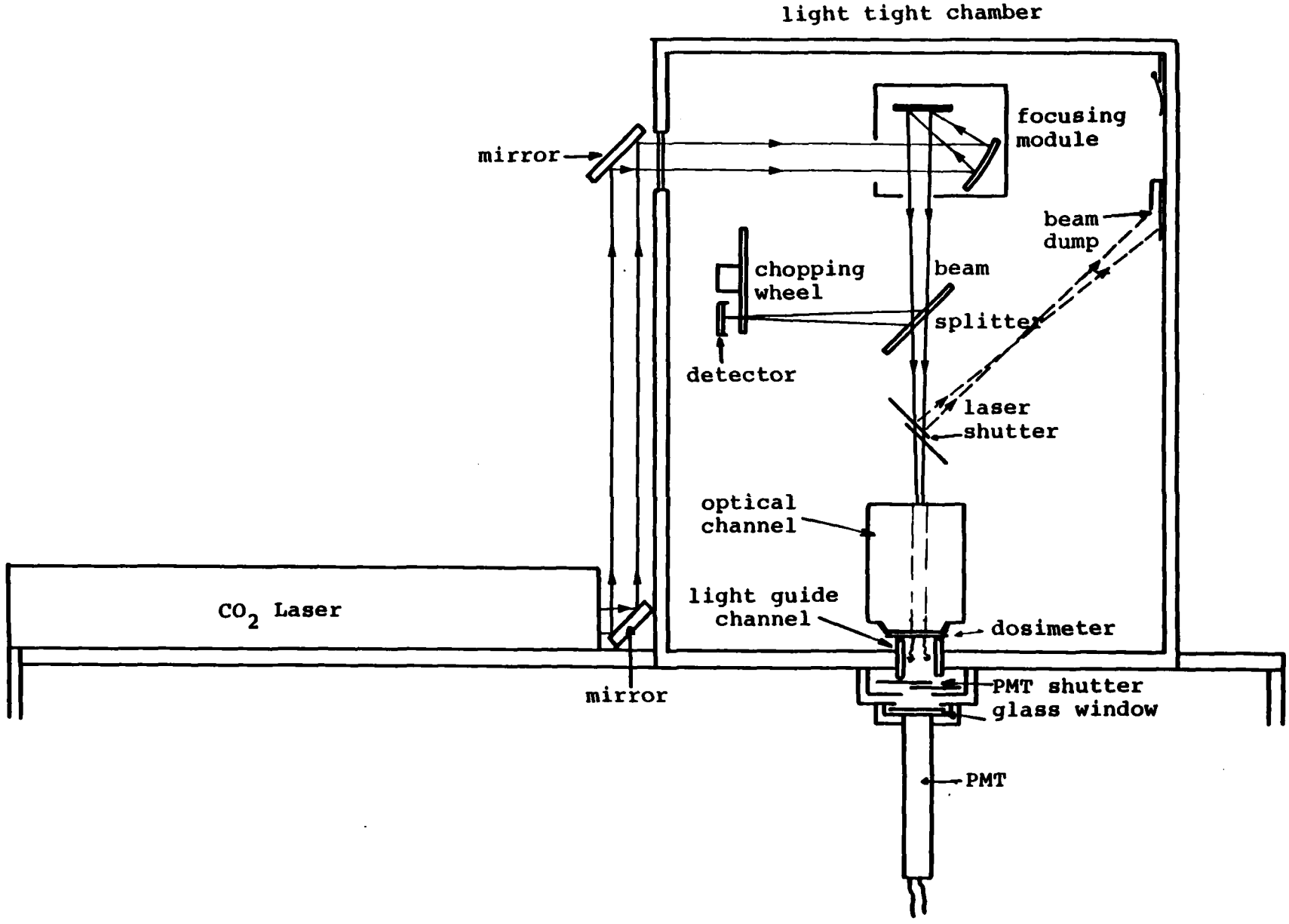
light tight chamber
focusing module
mirror
beam dump
chopping wheel
beam splitter
detector
laser shutter
optical channel
light guide channel
dosimeter
CO_2 Laser
mirror
PMT shutter
glass window
PMT

Fig. 1

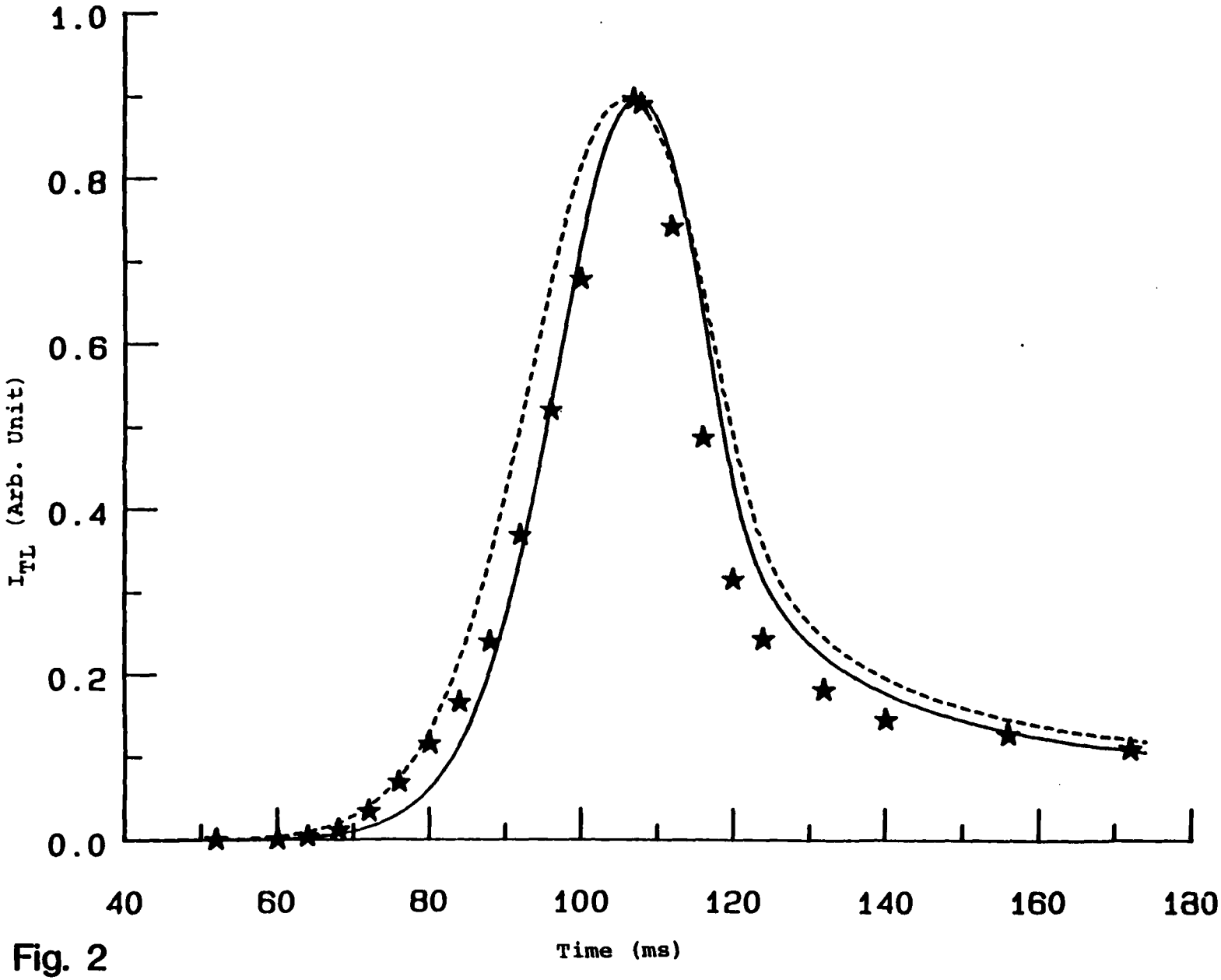

Fig. 2

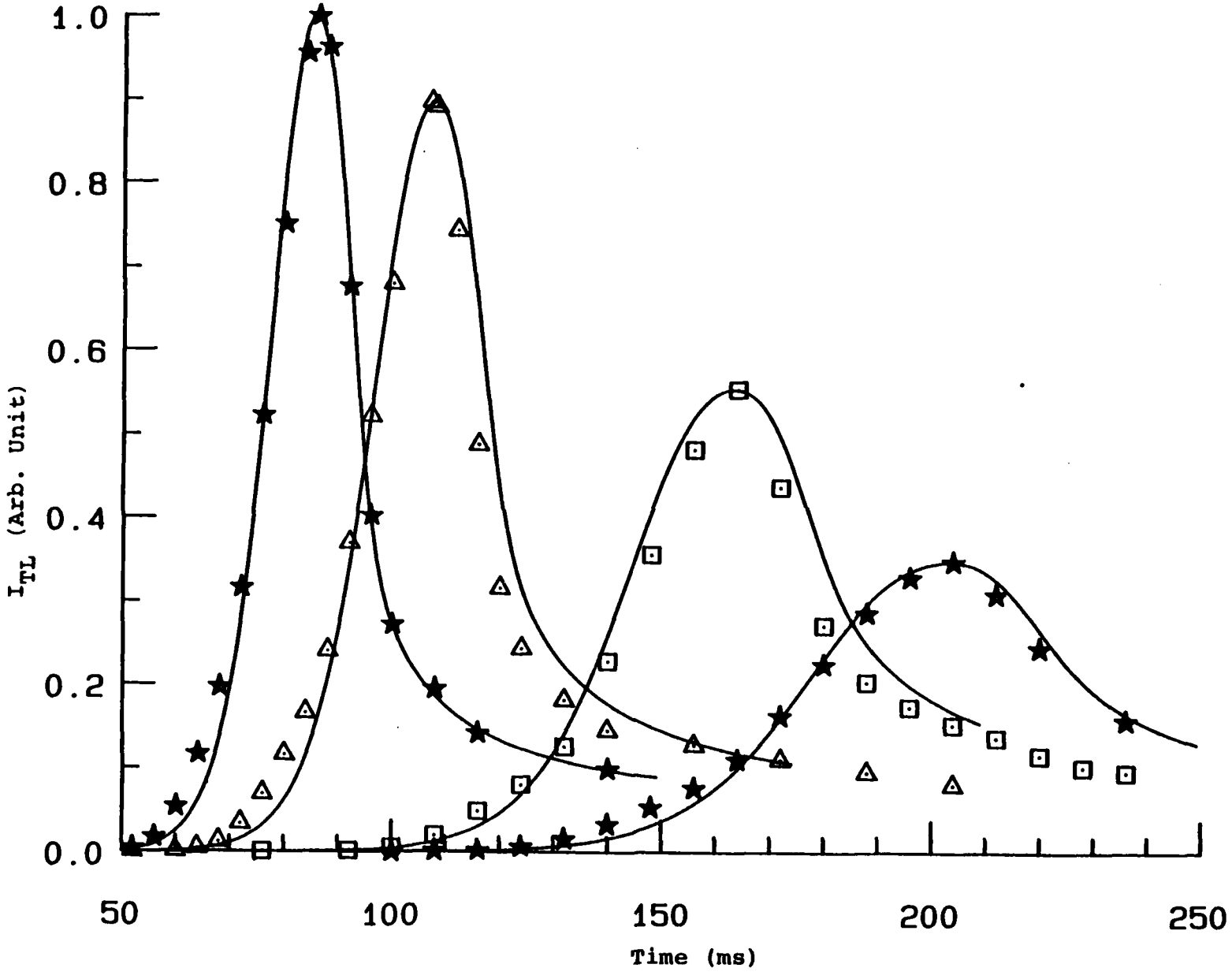

Fig. 3

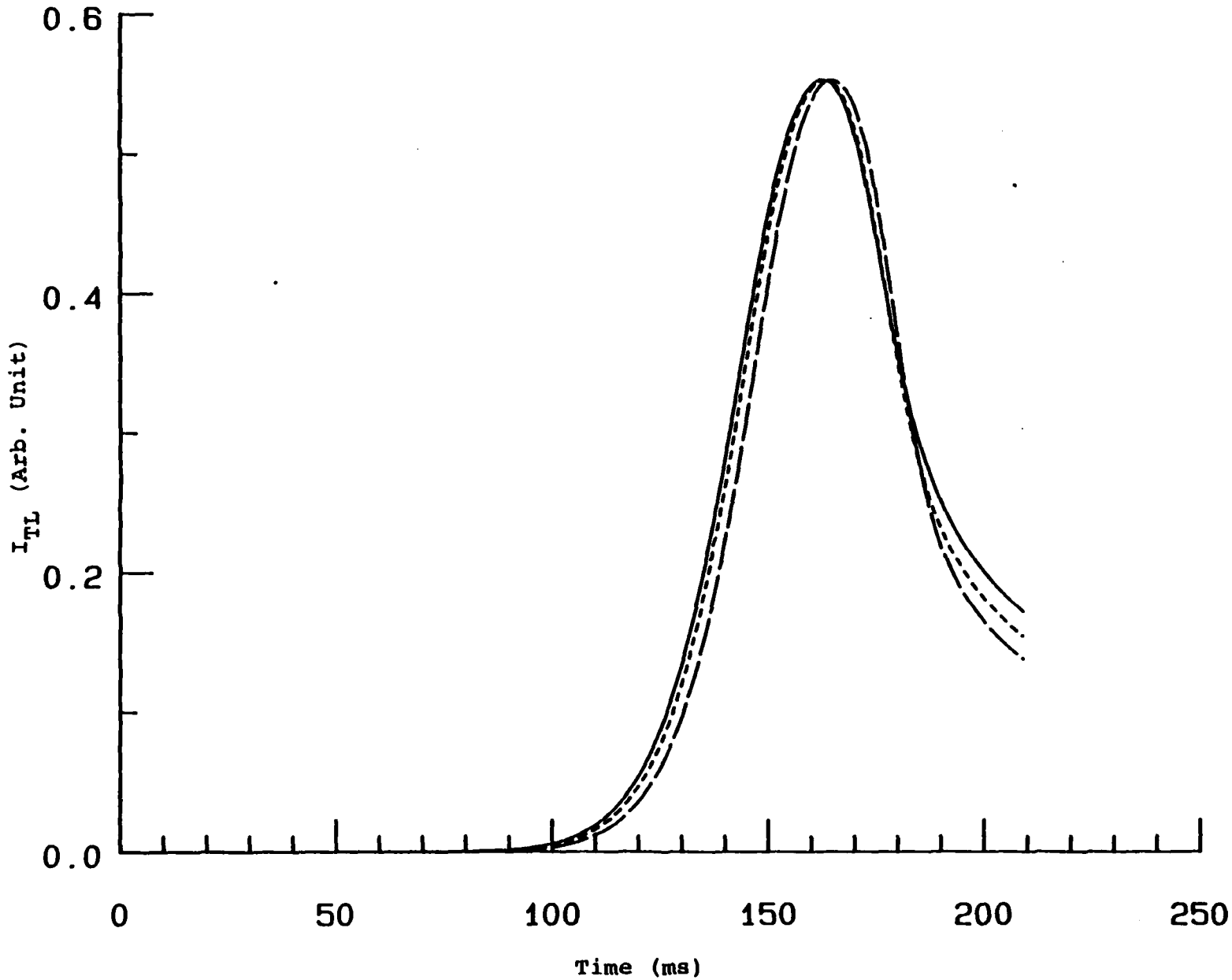

Fig. 4

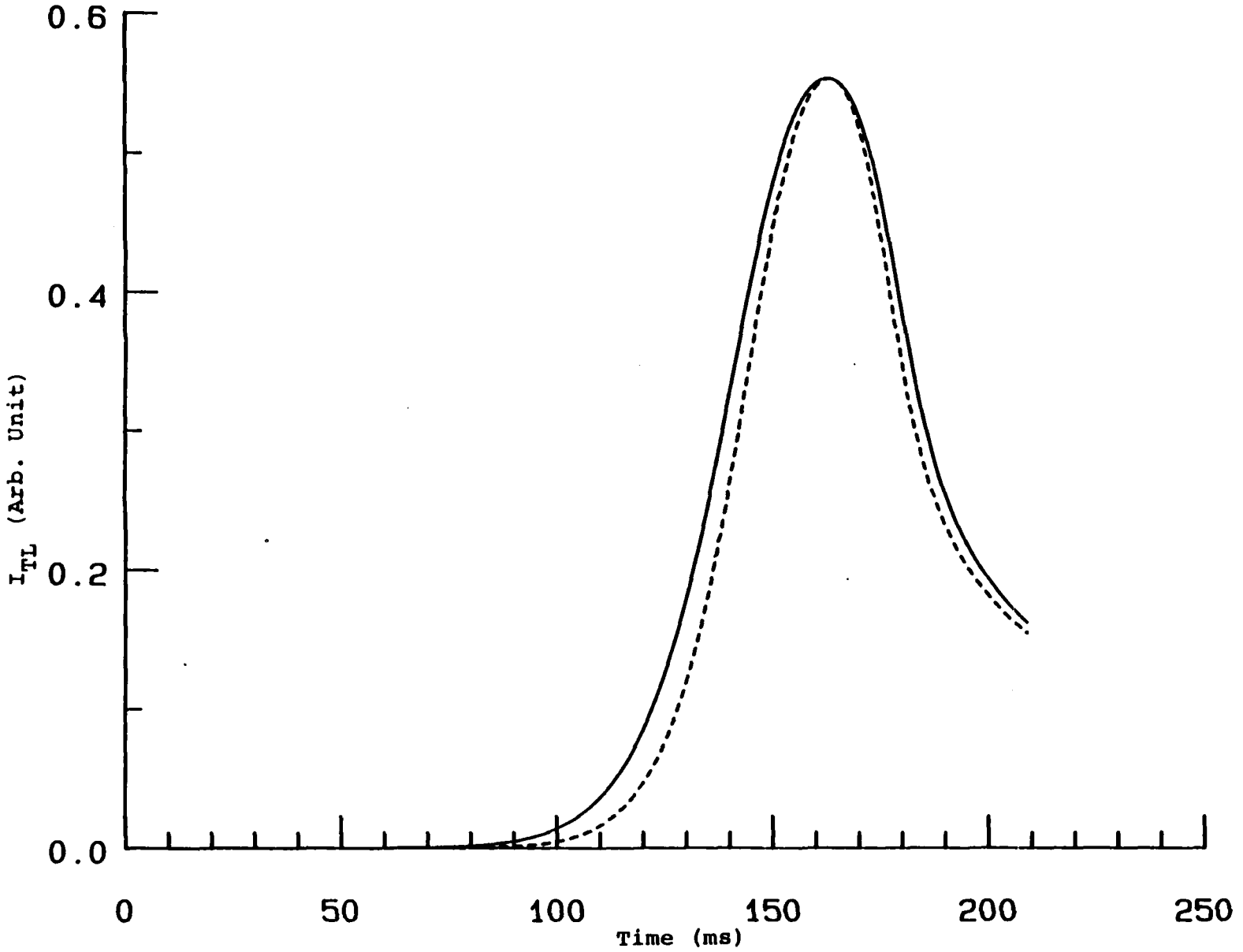

Fig. 5

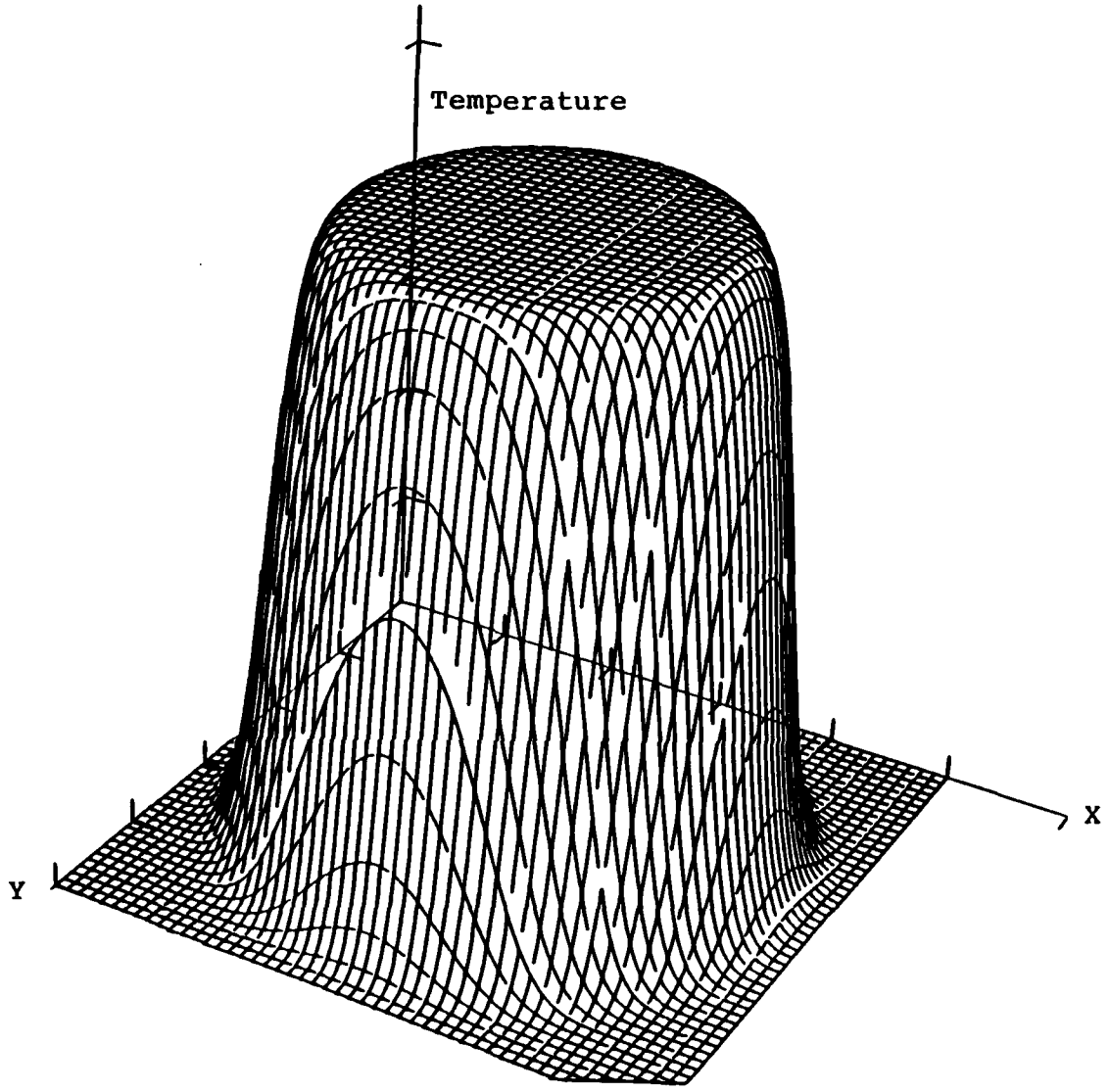

Fig. 6(a)

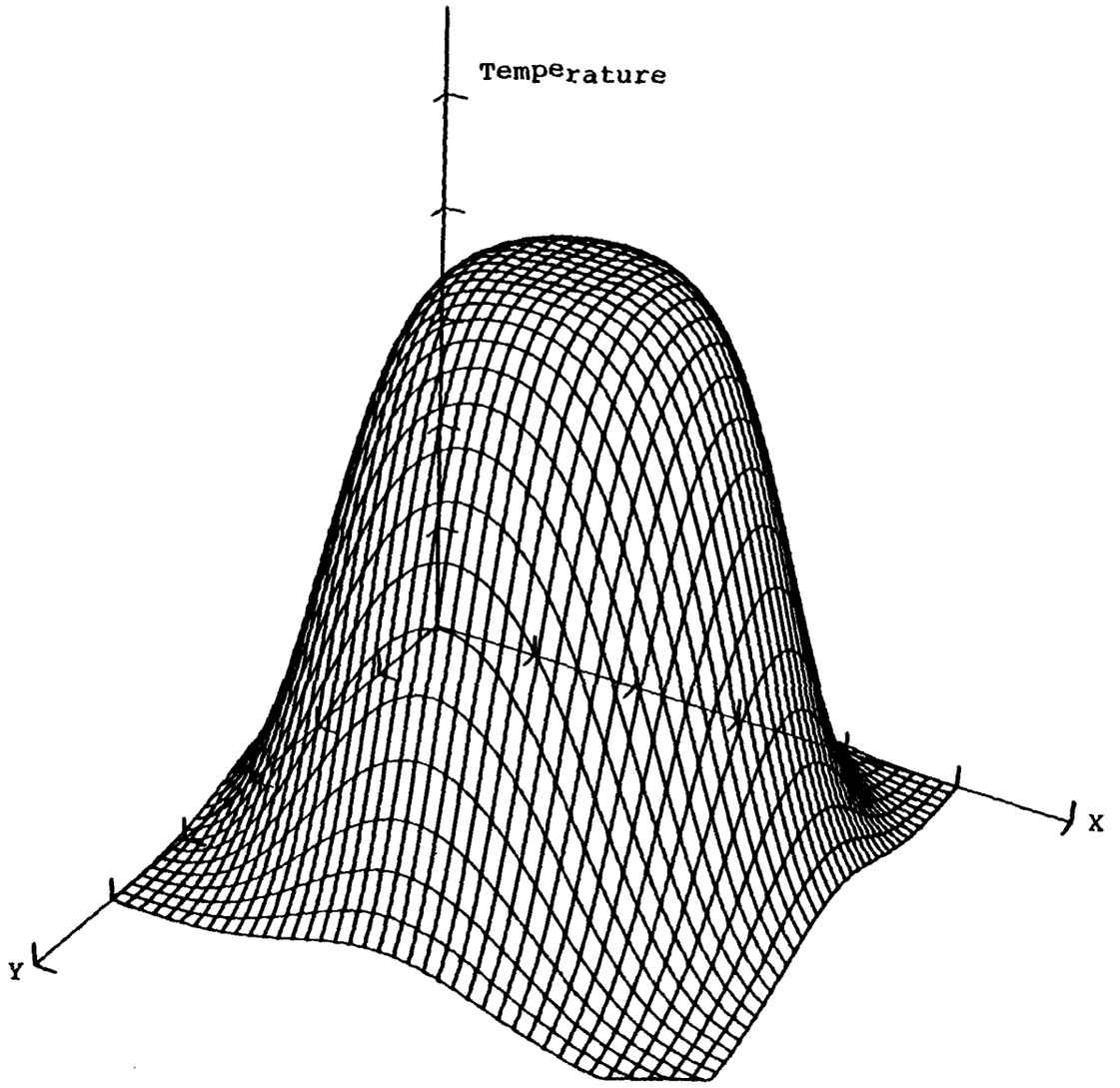

Fig. 6(b)

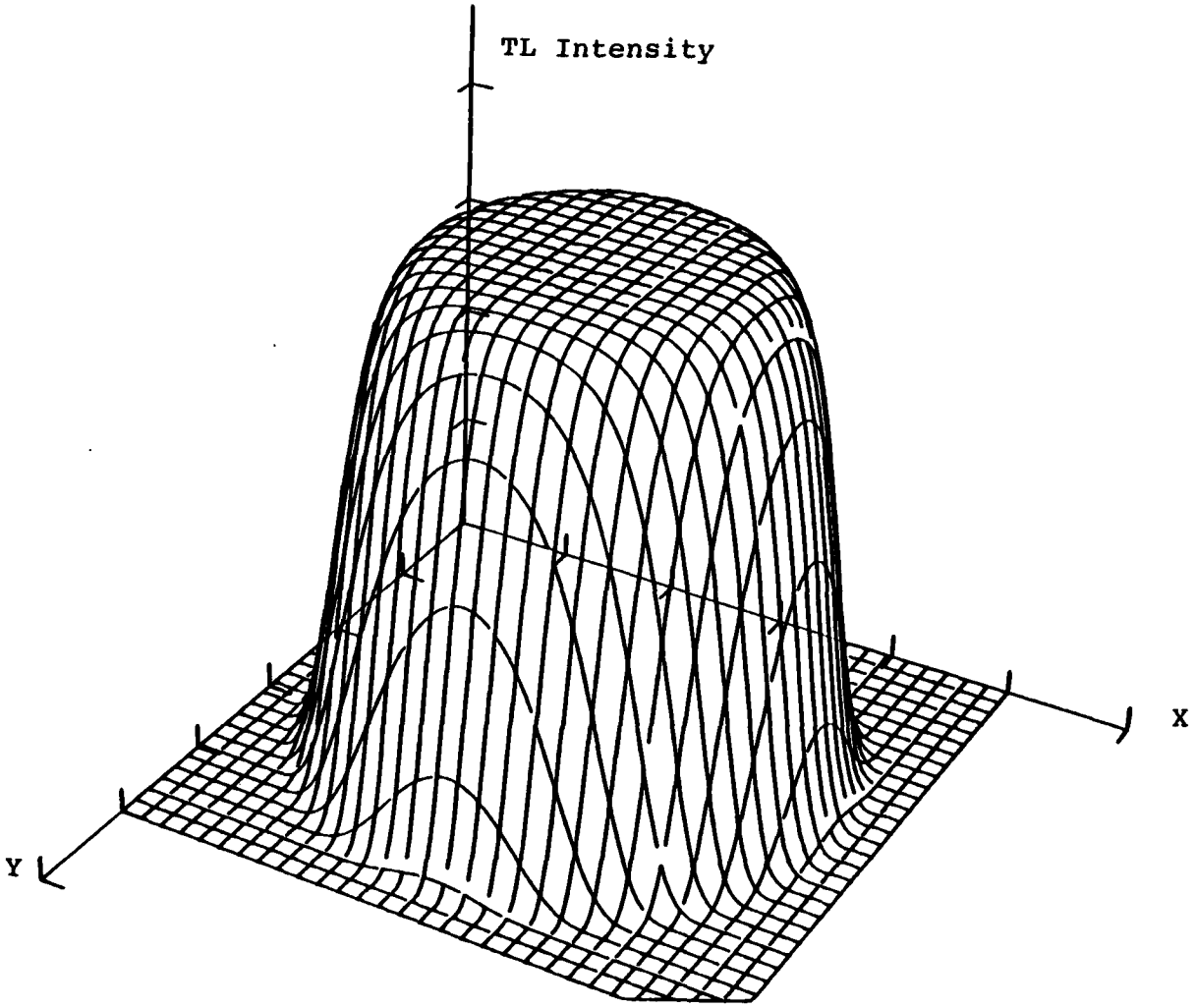

Fig. 7(a)

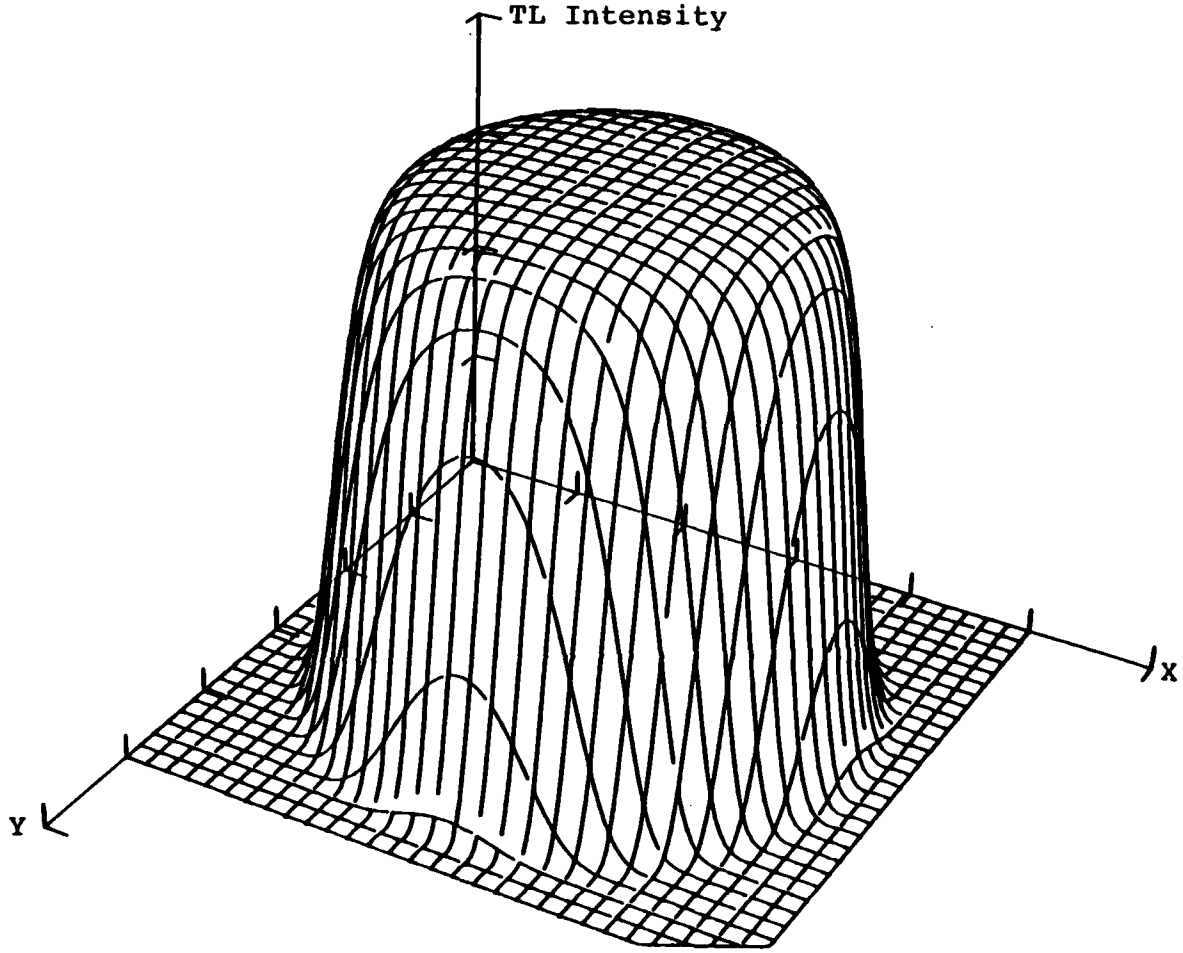

Fig. 7(b)

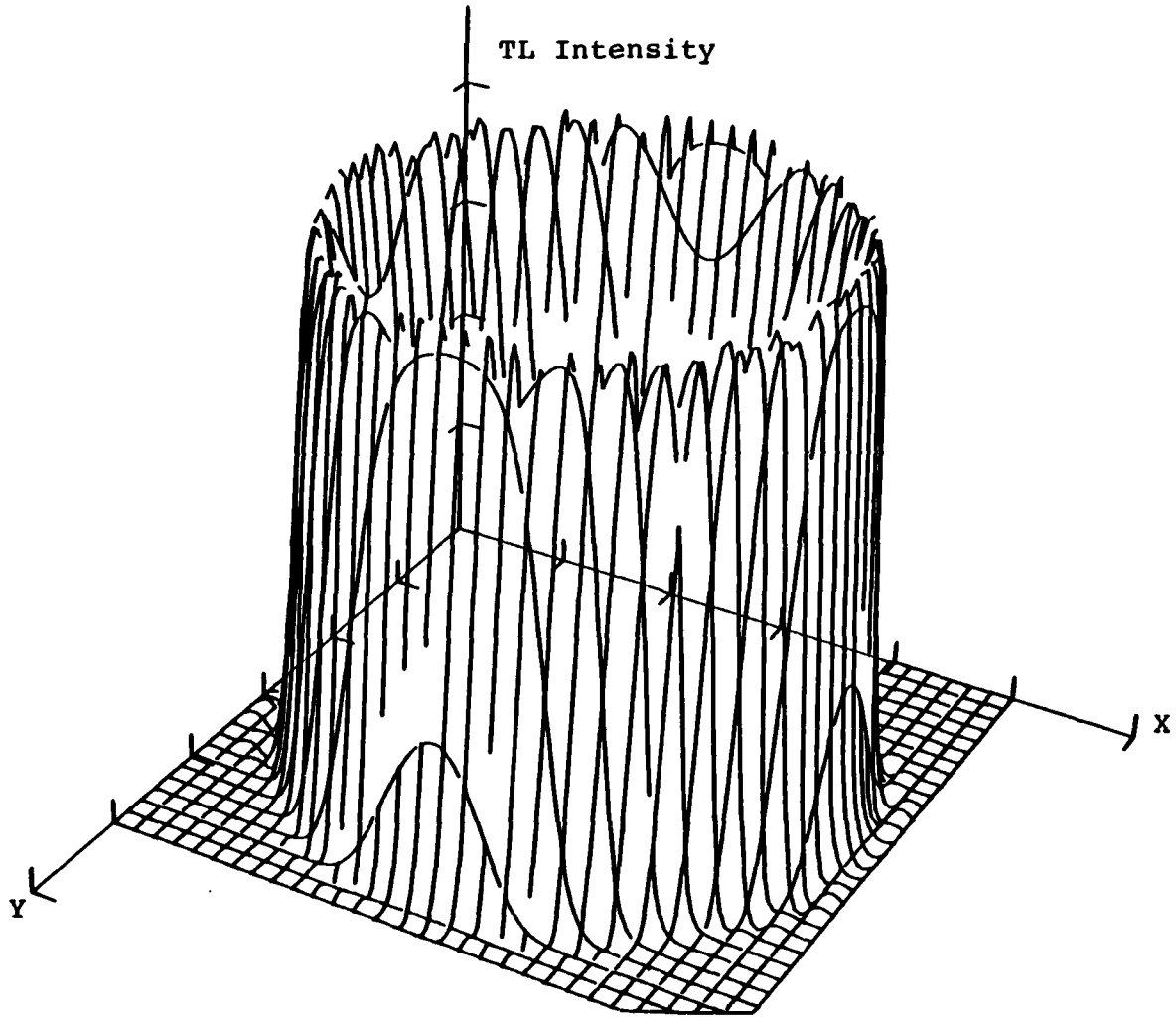

Fig. 7(c)

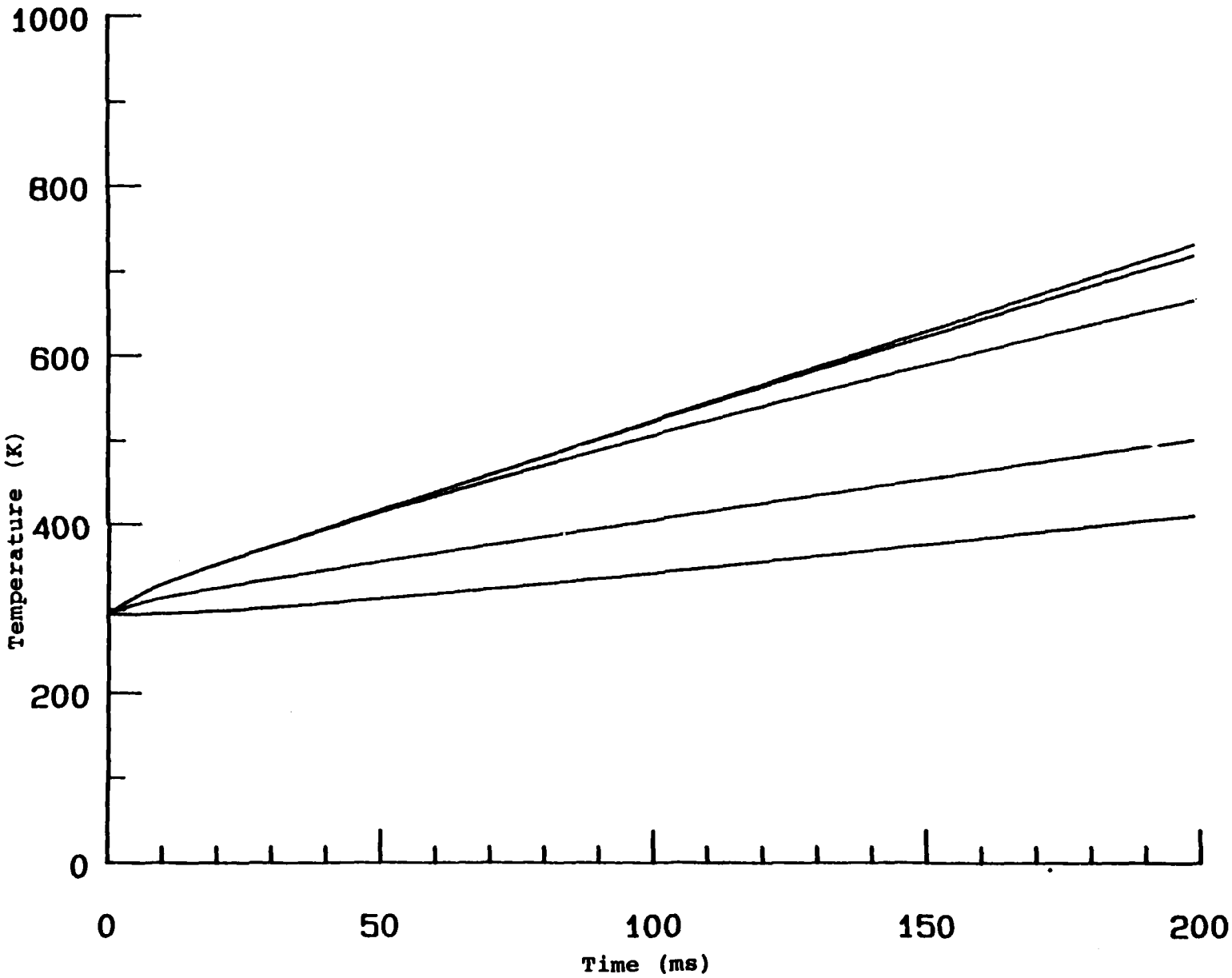

Fig. 8

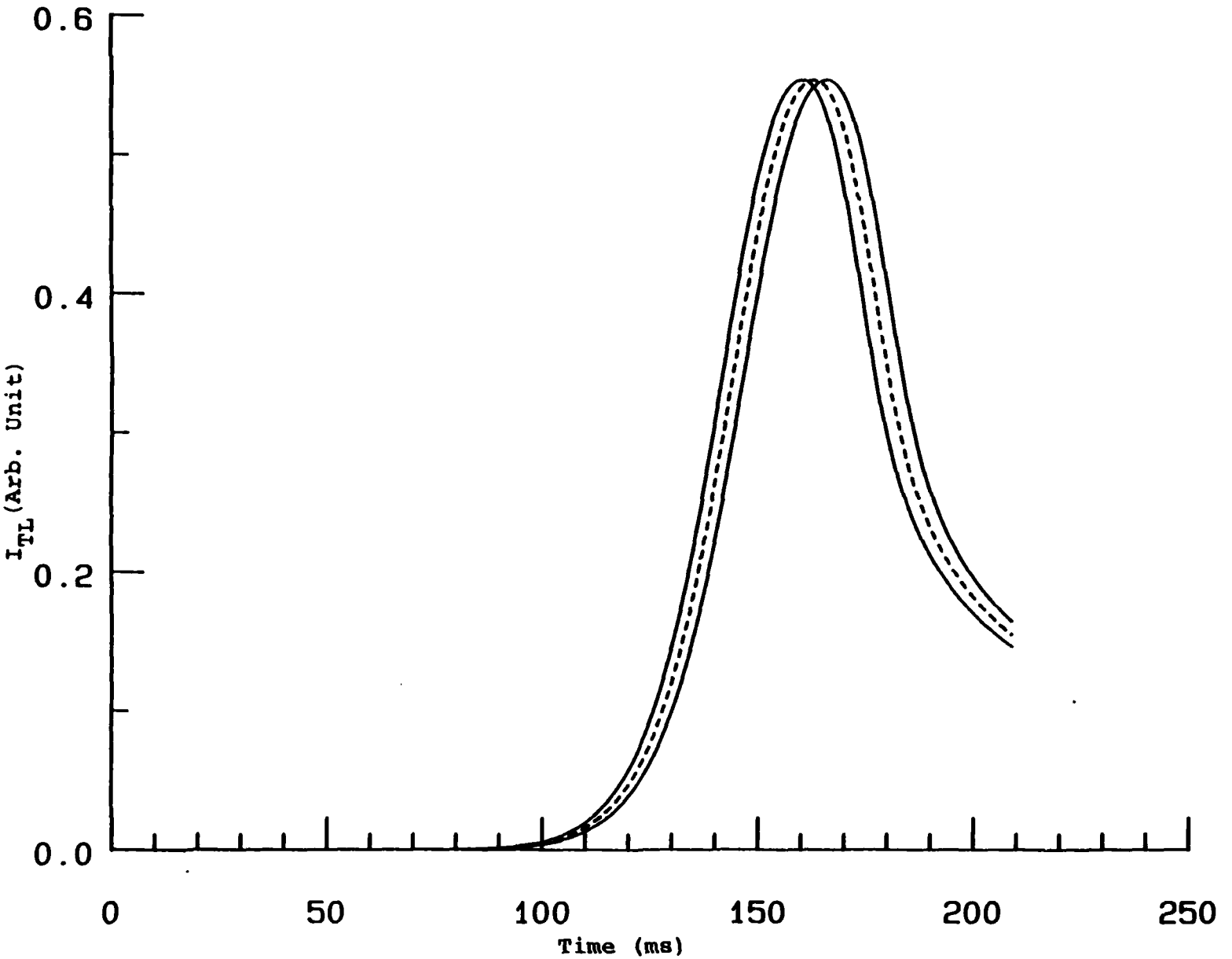

Fig. 9

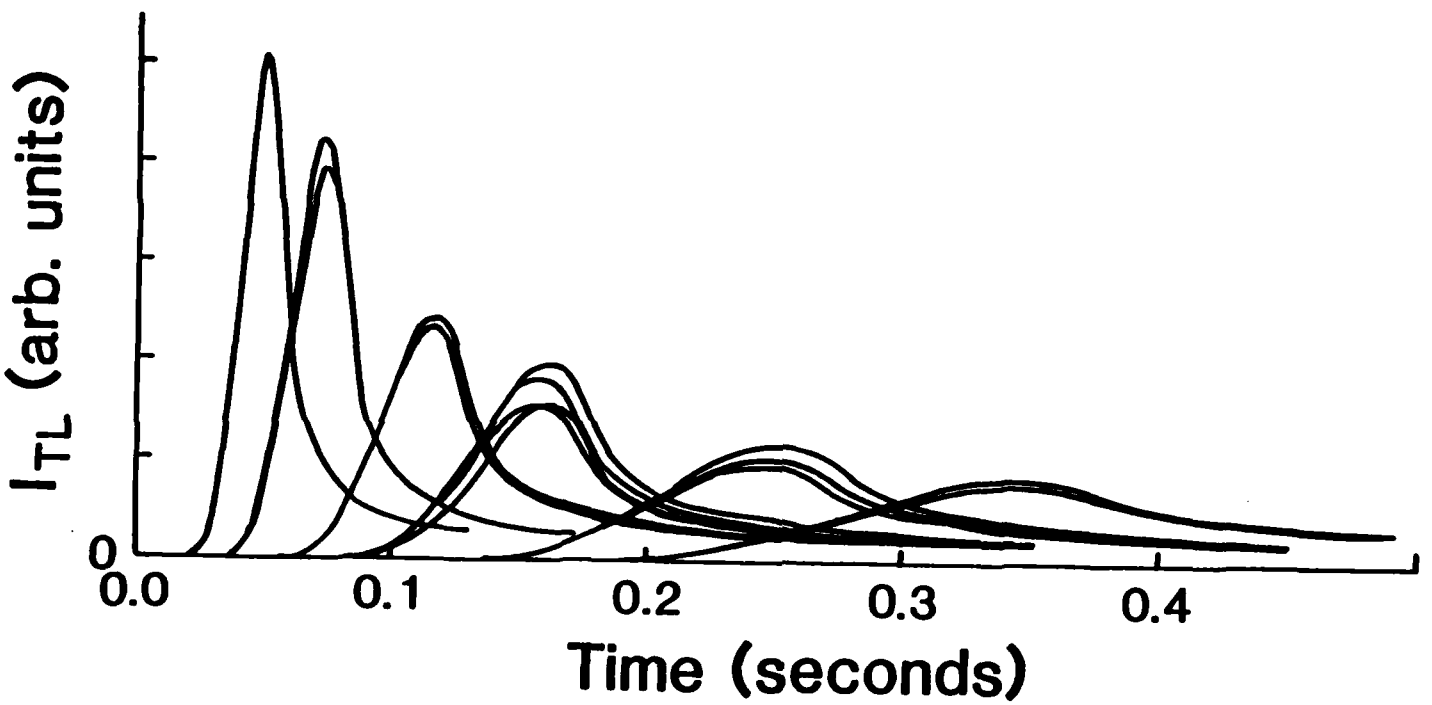

Fig. 10

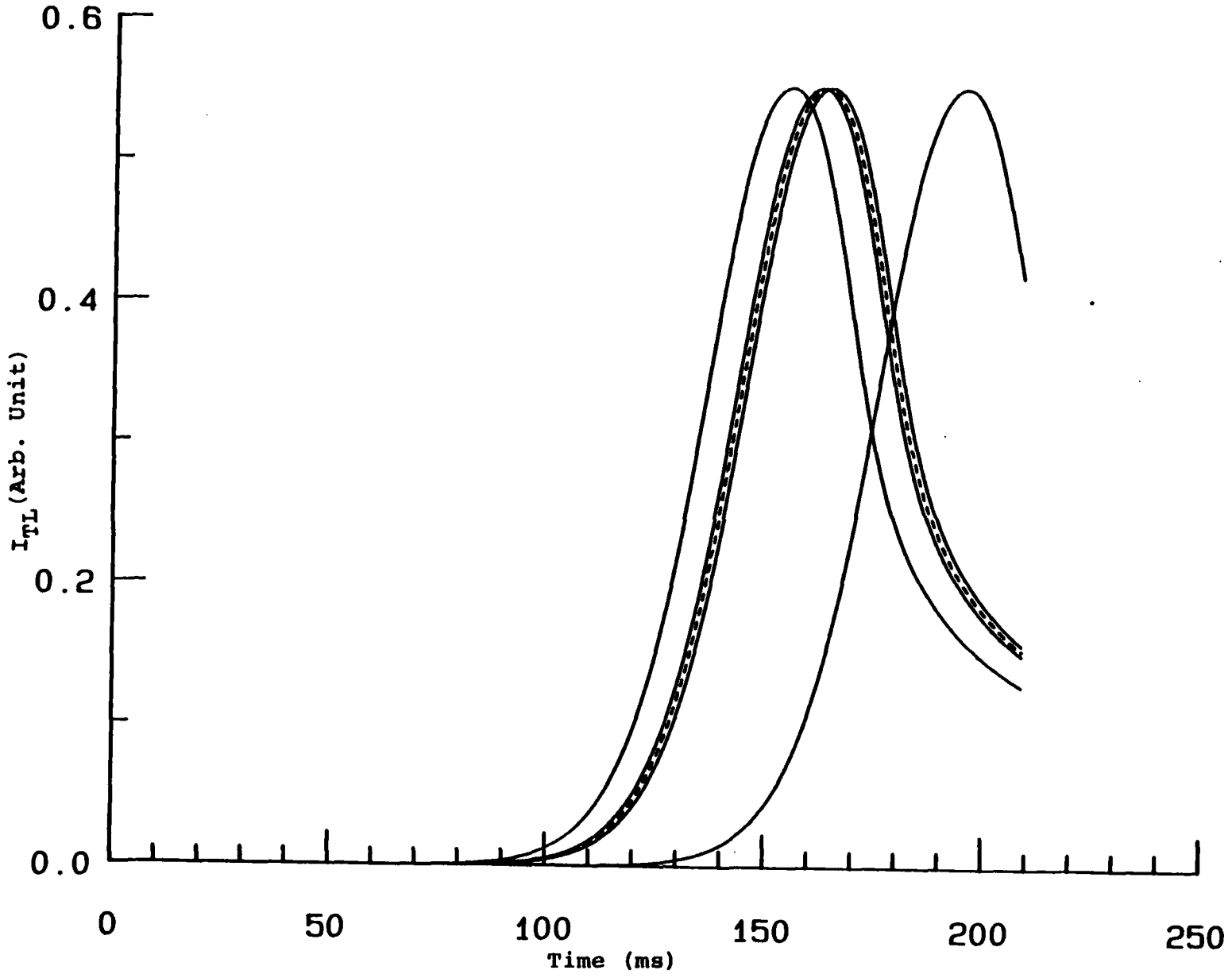

Fig. 11

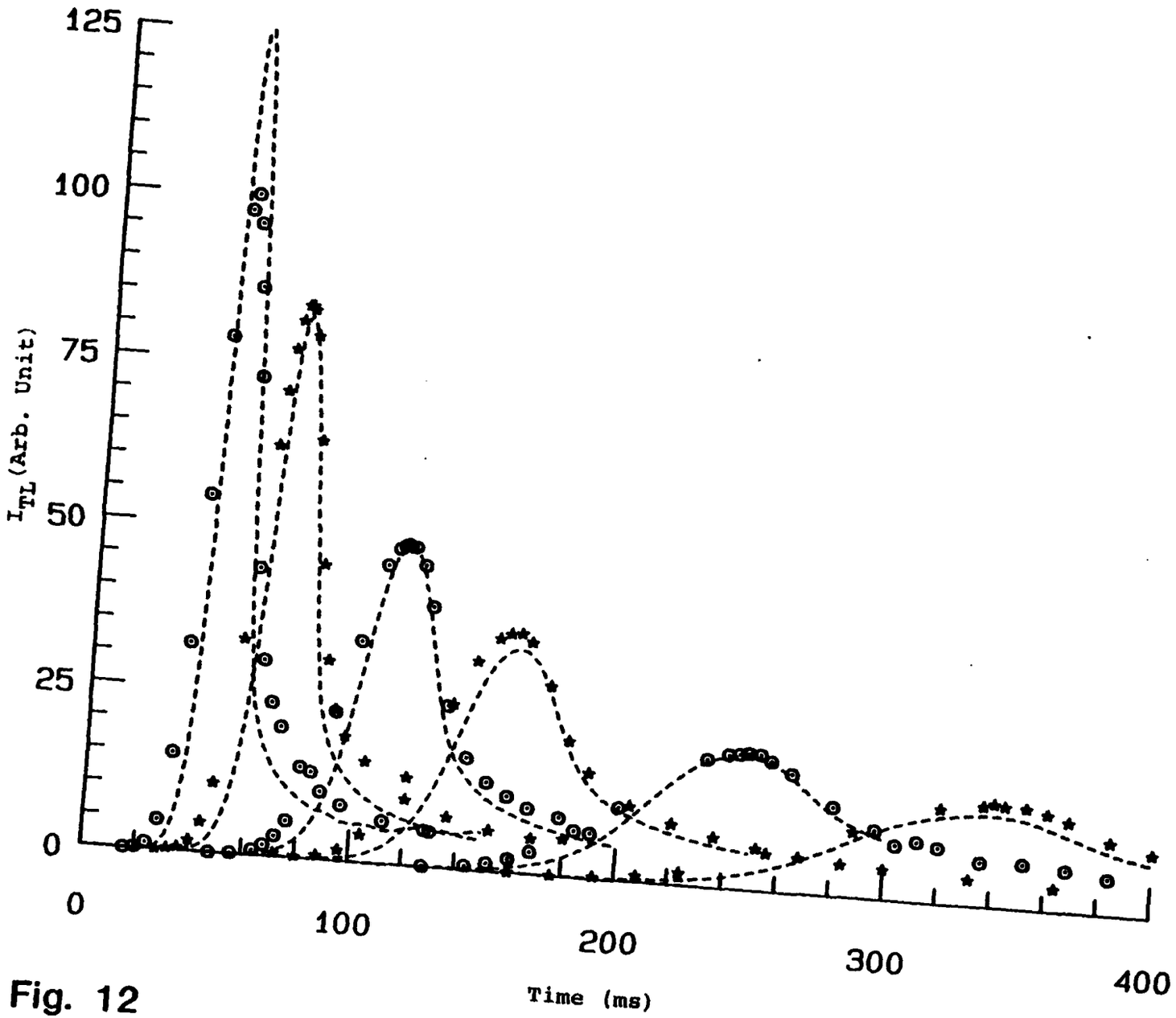

Fig. 12

DEVELOPMENT OF OPTICALLY STIMULABLE STORAGE PHOSPHORS FOR IMAGING OF NEUTRON DOSE DISTRIBUTIONS

I. INTRODUCTION

In studies that commenced in 1981 we have, in collaboration with Prof. J. Gasiot, University of Montpellier, France, established that certain optically stimulable phosphors can retain a fraction of the energy absorbed from ionizing radiation fields such as UV, x-rays, protons, etc. and that this energy can be released in form of visible luminescence on a time scale of about 100 ns when exposed to an infrared laser beam. Furthermore, the infrared stimulation spectrum of some of these phosphors turned out to overlap the emission wavelength of conventional Nd:YAG lasers. This finding pointed immediately to applications in real-time imaging of dose distribution [1], the most intriguing of which appeared to be neutron imaging for the purpose of non-destructive testing of large objects containing elements of low order number, e.g. polymers. The mode of operation one can envisage is the use of a so-called proton radiator in form of an approximately 1 mm thick polyethylene layer in front of the phosphor screen. The neutrons, generated in a conventional neutron generator rather than a reactor or a neutron source such as Pu-Be or 252 Cf (to keep the gamma component of the radiation as low as possible), produce knock-on protons in the proton radiator which in turn interact with the grains of the phosphor. In this process the electron traps are filled proportionally to the proton density. Thus, a latent image is stored which is released upon exposure to the stimulating IR laser beam. This beam will scan the phosphor and in this way produce a luminescence emission that is detected by a photomultiplier tube, digitized, and processed by a commercially available imaging processor. In contrast to other luminescence converter phosphors, the storage capability of the phosphors we investigate facilitates a mode of operation that might be called real-time or nearly real-time imaging with intermediate information up-dating: while a pixel or a part of phosphor screen is "read" by the scanning IR laser beam, the

radiation can already "imprint" new information on the section of the screen that is not exposed to the stimulating laser reading beam. The scanning laser beam is an ideal way to digitize the image on a pixel- by-pixel basis. For real-time scanning-type digitization to be possible, no luminescence overlapping the IR stimulated luminescence band from a pixel exposed to the IR laser beam can be allowed to be emitted from the entire screen. This is particularly true for the luminescenece emitted during exposure to the ionizing radiation. In other words, the luminescence emitted during and after exposure of the screen to the ionizing radiation must occur in an emission band that is different from the IR stimulated emission so that it can be completely blocked with filters from reaching the detector.

During examination of a large number of IR stimulable phosphors, mostly prepared and provided Prof. Gasiot for our use prior to this contract, we observed that certain samarium-cerium co-doped sulphides emit orange luminescence during UV excitation, but switch to a distincly green emission when exposed afterwards to IR. This more or less accidental observation formed the basis for the present study whose goal is to develop the phosphors for later use in nearly real-time neutron imaging.

Of course, the phosphor must posses certain properties to be a successful candidate for the future development of a complete neutron imaging system comprising a long "wish list". It is the purpose of the work performed under this contract to identify such suitable phosphors and to establish their basic physical characteristics vis-a-vis the goal of near real-time neutron imaging.

The ideal phosphor must:

1. emit a different luminescence spectrum during exposure to the radiation whose distribution is to be imaged as compared to the spectrum emitted during image retrieval by the scanning IR laser beam,

2. be efficiently stimulable by a conventional commercially available laser whose wavelength must be such as to not cause a signal in the detector

used for signal generation with the IR stimulated luminescence, i.e. the IR stimulation spectrum must be different from the IR-stimulated luminescence emission spectrum,

3. be capable of retaining an acceptable fraction of the energy from the ionizing radiation (most importantly neutron-generated knock-on protons), and efficiently convert the stored energy to luminecence upon stimulation by the IR laser beam,

4. be capable of a large dynamic range, that is the dose proportionality must have a useful range of at least four orders of magnitude.

While it is well known that the conversion efficiency of energy absorbed from the radiation field to visible luminescence can approach several percent and the IR stimulation spectra and emission spectra of a number of phosphors have the desired properties listed above under 2., producing a phosphor that emits a different luminescence spectrum during exposure to the ionizing radiations as compared to the one generated during IR stimulation presented a considerable challenge. As this property is the most important one, we have concentrated on it during the contract period from 7-15-85 through 3-15-86.

The phosphors we have selected for this study are MgS:Ce(0.1%). Sm(0.05%) and CaS:Ce(0.1%),Sm(0.05%). They represnt the best phosphors prepared to-date. In the following we will first decribe the method of their preparation, which has emerged in extensive trials with differnt preparation parameters. Thereafter, we report on the spectral, decay and storage properties of the luminescence.

radiation can already "imprint" new information on the section of the screen that is not exposed to the stimulating laser reading beam. The scanning laser beam is an ideal way to digitize the image on a pixel- by-pixel basis. For real-time scanning-type digitization to be possible, no luminescence overlapping the IR stimulated luminescence band from a pixel exposed to the IR laser beam can be allowed to be emitted from the entire screen. This is particulartly true for the luminescenece emitted during exposure to the ionizing radiation. In other words, the luminescence emitted during and after exposure of the screen to the ionizing radiation must occur in an emission band that is different from the IR stimulated emission so that it can be completely blocked with filters from reaching the detector.

During examination of a large number of IR stimulable phosphors, mostly prepared and provided Prof. Gasiot for our use prior to this contract, we observed that certain samarium-cerium co-doped sulphides emit orange luminescence during UV excitation, but switch to a distincly green emission when exposed afterwards to IR. This more or less accidental observation formed the basis for the present study whose goal is to develop the phosphors for later use in nearly real-time neutron imaging.

Of course, the phosphor must posses certain properties to be a successful candidate for the future development of a complete neutron imaging system comprising a long "wish list". It is the purpose of the work performed under this contract to identify such suitable phosphors and to establish their basic physical characteristics vis-a-vis the goal of near real-time neutron imaging.

The ideal phosphor must:

1. emit a different luminescence spectrum during exposure to the radiation whose distribution is to be imaged as compared to the spectrum emitted during image retrieval by the scanning IR laser beam,

2. be efficiently stimulable by a conventional commercially available laser whose wavelength must be such as to not cause a signal in the detector

2. CaF sub2 and KBr are inefficient fluxes.
3. NaCL and NH sub 4 Cl are more efficient than MgCL sub 2 and BaCl sub 2, but all work fine.
4. Increasing the flux concentration improves IR stimulability while simultaneously decreasing the Sm luminous efficiency.
5. The most effective flux concentrations turned out to be in the range from 0.5% to 4.0%.

III. LUMINESCENCE PROPERTIES OF CE/SM CO-DOPED MAGNESIUM SULPHIDE AND CALCIUM SULPHIDE

The properties investigated to-date include the IR stimulation spectra, the emission spectra during UV excitation, during simultaneous UV excitation and IR stimulation, and during IR stimulation at various storage times after UV excitation. All these experiments were carried out with the aid of a Princeton Applied Research optical multichannel analyser (type: OMA III).

Initial experiments have also been performed on the decay times of the luminescence emission, but a detailed investigation of the IR stimulation properties (response time, decay time as a function of power density, and the experimental conditions required to completely empty the traps and, thus, quench the stored image information by IR stimulation) has not yet been executed. It requires the use of a Nd:YAG laser system, which will be available for these experiments after May 15, 1986.

1. Luminescence Emission Spectrum during UV Excitation

Exposure of the phosphor layers to the 253.7 nm mercury line (mercury penlight plus narrow band interference filter) yields the emission spectra of Figs. 1 and 2. Both exhibit the characteristic lines of Sm and a broad unresolved band due to Ce [2].

II. PHOSPHOR PREPARATION

Reproducible results in preparing IR stimulable phosphors can only be achieved by careful process control. Our preparation facility consistes of a Lindberg three zone tube furnace and specially designed gas handling equipment.

Phosphor preparation includes the following steps:

1. Reduction of MgSO4 or CaSO4 to MgS or CaS in an atmosphere of dry nitrogen and carbon disulphide. Reagent grade nitrogen is dried by bubbling through fuming sulfuric acid. Carbon disulfide is admixed by bubbling this dried gas through liquid CS sub 2. This gas mixture enters the aluminum oxide tube in the furnace, in the center of which the powders to be reduced are placed in quartz boats or aluminum oxide containers. Quartz permits faster cooling times, a feature necessary for faster preparation of MgS phosphors. The reduction process requires heating the material in the CS sub 2 /N sub 2 atmosphere at 850°C for one hour.

2. The sulphides produced in step 1. are intimately mixed with the dopants (in form of samarium oxide and cerium oxide), the flux agent (see figures for details), and additional sulfur.

3. This mixture is fired in dry nitrogen gas at 1050°C for MgS and at 1220°C for CaS. After cooling to 850°C, the CS sub 2 gas is added to the nitrogen. The total firing cycle requires two hours for proper diffusion of the dopants through the powder grains.

To produce these best-effort phosphors, carefully searching for the optimum heating cycles was required. In addition, we had to experiment with various concentrations of the dopants as well as different fluxing agents of various concentrations. Fluxes tested included CaF sub 2, KBr, NH sub 4Cl, NaCl, MgCl sub 2, and BaCl sub 2. These flux tests can be summarized as follows:

1. Sm requires no flux for efficient diffusion.

In view of the anticipated application of both phosphors in radiation imaging and the requirement that IR stimulation must be possible with a cost-efficient scanning-beam laser system such as a Nd:YAG laser, the range of IR wavelengths that can stimulate the luminescence emission by releasing the electrons from the storage traps is of particular interest. We have measured these spectra with an IR monochromator (grating blazed for 1.3 um). The results, still preliminary in detail(e.g. the apparent structure is unconfirmed) are presented in Figs. 7 and 8. As hoped, the stimulation spectra for both phosphors peak at or near the 1.06 um wavelength of the Nd:YAG laser photons.

5. Decay and Storage Properties

Since admixtures of both spectral components in the UV excitation and IR stimulation spectra are always present and complete spectral discrimination in the excitation and stimulation mode of the imaging process does not appear feasible with these phosphors, we have investigated the possibility of near real-time imaging. Here, the excitation with knock-on protons or other ionizing radiation does not occur during IR stimulation with the scanning laser beam. Instead, the excitation source (i.e. the neutron generator beam) is interrupted during the scanning process. Since we fully expect the response time to the scanning beam to be very fast, rapid "reading" of the stored image with a sufficiently intense Nd:YAG laser beam [1] is possible. Thus, the image can be updated in as little time as it takes to store a new image (which depends of course on the neutron fluence) plus the times required for the complete decay of the undesired spectral component present during UV excitation (in our case the Ce band) and for reading with the scanning laser beam. As was shown previously, the reading time can be much less than a second [1]. We expect the imaging system to provide an updated image in less then a few seconds.

Therefore, knowledge of the decay time of the undesired spectral component, the Ce band present during UV stimulation, is of paramount importance. We have

2. Luminescence Emission Spectra during Simultaneous UV Excitation and IR Stimulation

An indication of the effectiveness of IR stimulation may be had by simultaneously exposing the phosphor to UV and IR. The IR illumination was obtained from a Kodak slide projector (300 Watt quartz-halogen lamp, heat filter replaced by 2 mm thick polished but uncoated silicon window to block all radiation below 900 nm wavelength). Figs. 3 and 4 demonstrate that IR exposure in addition to 253.7 nm UV excitation significantly enhances the Ce emission band, but does not affect the Sm lines.

3. IR Stimulated Luminescence Emission Spectra

After filling the electron storage traps by UV excitation, exposure to IR causes luminescence emission whose spectra are shown in Figs. 5 and 6. They clearly demonstrate that the orange component that is so dominant during UV excitation is now very weak compared to the green Ce emission band. This is precisely the hoped for property of the phosphors we have developed for eventual later application in radiation imaging. In comparing the UV excited luminescence with the IR stimulated one, it also becomes clear that the anticipated complete separation of these spectra is not present. Both types always contain components of both the Sm and the Ce emission spectra. Complete separation would have meant that real-time imaging is feasible. In light of the admixture of the Sm lines in the IR stimulated spectra and of the Ce band in the UV excited ones, only "nearly real-time" imaging appears possible. We will discuss this point in more detail below.

4. IR Stimulation Sectra

FIGURE CAPTIONS

Fig. 1
Luminescence emission spectrum for MgS:Ce(0.1%),Sm(0.05%)+2% Cl flux [standard MgS phosphor] during excitation with 253.7 nm UV. Spectral assignment from Ref.1

Fig.2
Luminescence emission spectrum for CaS:Ce(0.1%),Sm 0.05%)+2% Cl flux [standard CaS phosphor] during excitation with 253.7 nm UV. Spectral assignment as in Fig.1

Fig.3
Luminescence emission from the standard MgS phosphor obtained by simultaneous excitation with 253.7 nm UV and stimulation with broadband IR (quartz halogen lamp plus 5 mm thick Si filter)

Fig. 4
Same as Fig. 3 for standard CaS phosphor

Fig. 5
Luminescence emission spectrum from the standard MgS phosphor after excitation with 253.7 nm UV and during subsequent stimulation with broadband IR. Note the difference compared to Figs. 1 and 3

Fig.6
Same as Fig. 5 for standard CaS phosphor. Compare with Figs. 2 and 4

Fig. 7
Spectral distribution of IR photons capable of stimulating the standard MgS phosphor after UV excitation. The intensity is a relative measure of the effectiveness of a given wavelength for IR stimulation.

studied the spectal dependance of the decay after UV excitation with the time resolution of approximately 300 ms possible with the OMA III system in its present configuration. Figure 9 indicates that the Ce luminescence has completely decayed in less than 300 ms. A gated OMA detector must be employed to improve the time resolution. This option is presently not available in our laboratory.

For applications where weaker excitation sources must be employed or storage of the latent image is desired, the storage time after excitation must be known. We have studied the response to a given IR stimulation radiation after excitation for a fixed time with a constant UV source. The results shown in Figs. 10 and 11 indicate that at room temperature storage times up to one hour (and possibly much longer) are possible without significant loss of the stored image information.

REFERENCES

1. J. Gasiot and P. Braunlich, Appl. Phys. Let. 40. 376 (1982)

2. S. P. Keller, Phys. Rev. 29, 180 (1957)

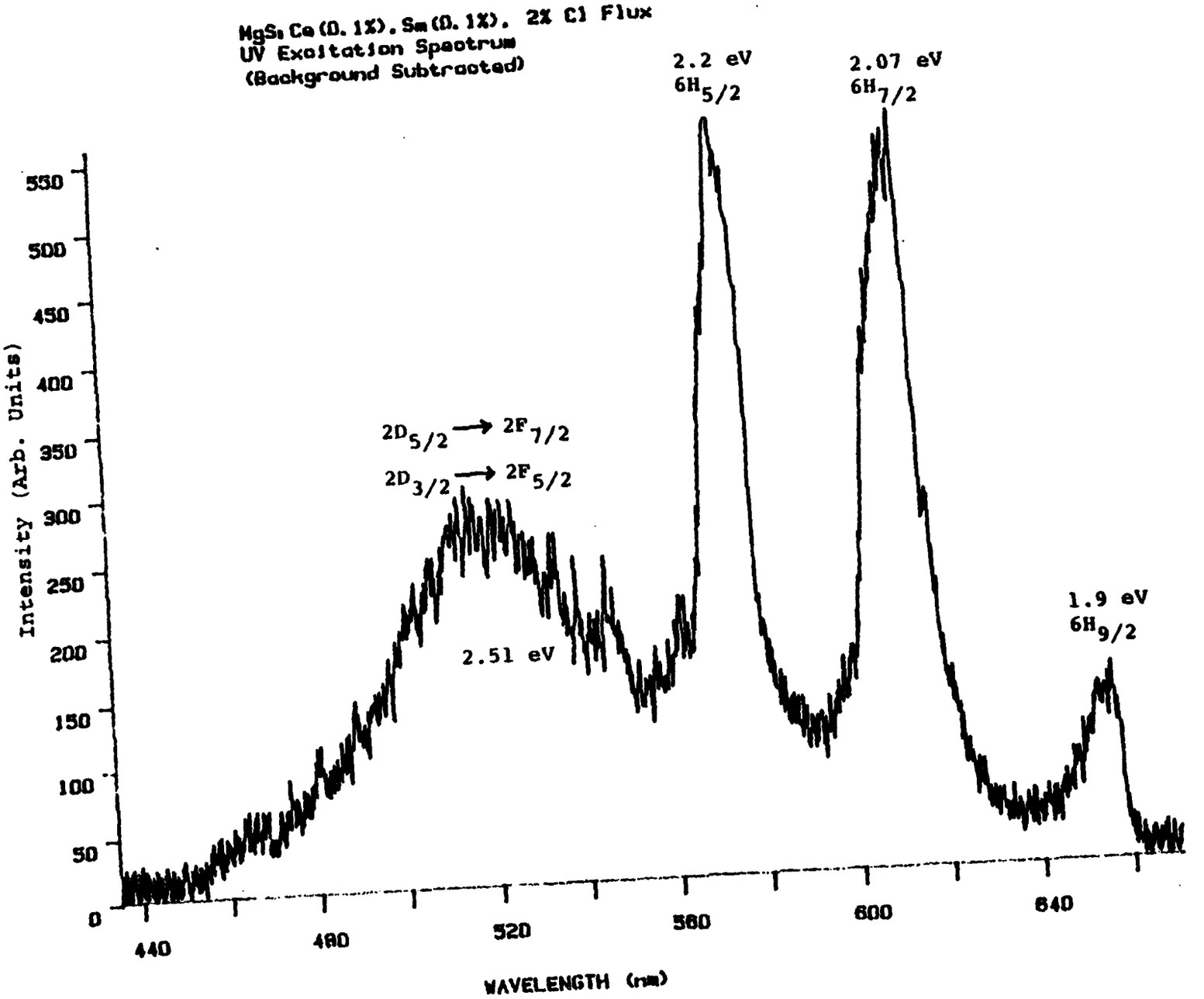
MgS: Ce(0.1%), Sm(0.1%), 2% Cl Flux
UV Excitation Spectrum
(Background Subtracted)
2.2 eV
6H5/2
2.07 eV
6H7/2
2D5/2 → 2F7/2
2D3/2 → 2F5/2
2.51 eV
1.9 eV
6H9/2
Intensity (Arb. Units)
0
50
100
150
200
250
300
350
400
450
500
550
440
480
520
560
600
640
WAVELENGTH (nm)

Fig. 1

Fig.8
Same as Fig.7 but for standard CaS phosphor

Fig. 9
Decay of the luminescence emission from the standard MgS phosphor after UV excitation. The Ce emission has completely decayed after less than 300 ms.

Fig. 10
Test of storagebility at room temperature of the energy deposited during UV excitation. The standard MgS phosphor was excited for a fixed time with 253.7 nm UV photons. The luminescence emission during IR stimulation was measured after the storage time indicated on the curves, which are offset for easier identification. The sharp rise of these response curves coincides with the onset of exposure to the broadband IR stimulation radiation. The increase in signal up to 30 min storage time is real and reproducible. At room temperature the stored signal decreases only after storage times of 60 min. or more.

Fig. 11
Same as in Fig. 10 but for the standard CaS phosphor. Note the significant decrease of the stored signal after only a few minutes of storage at room temperature.

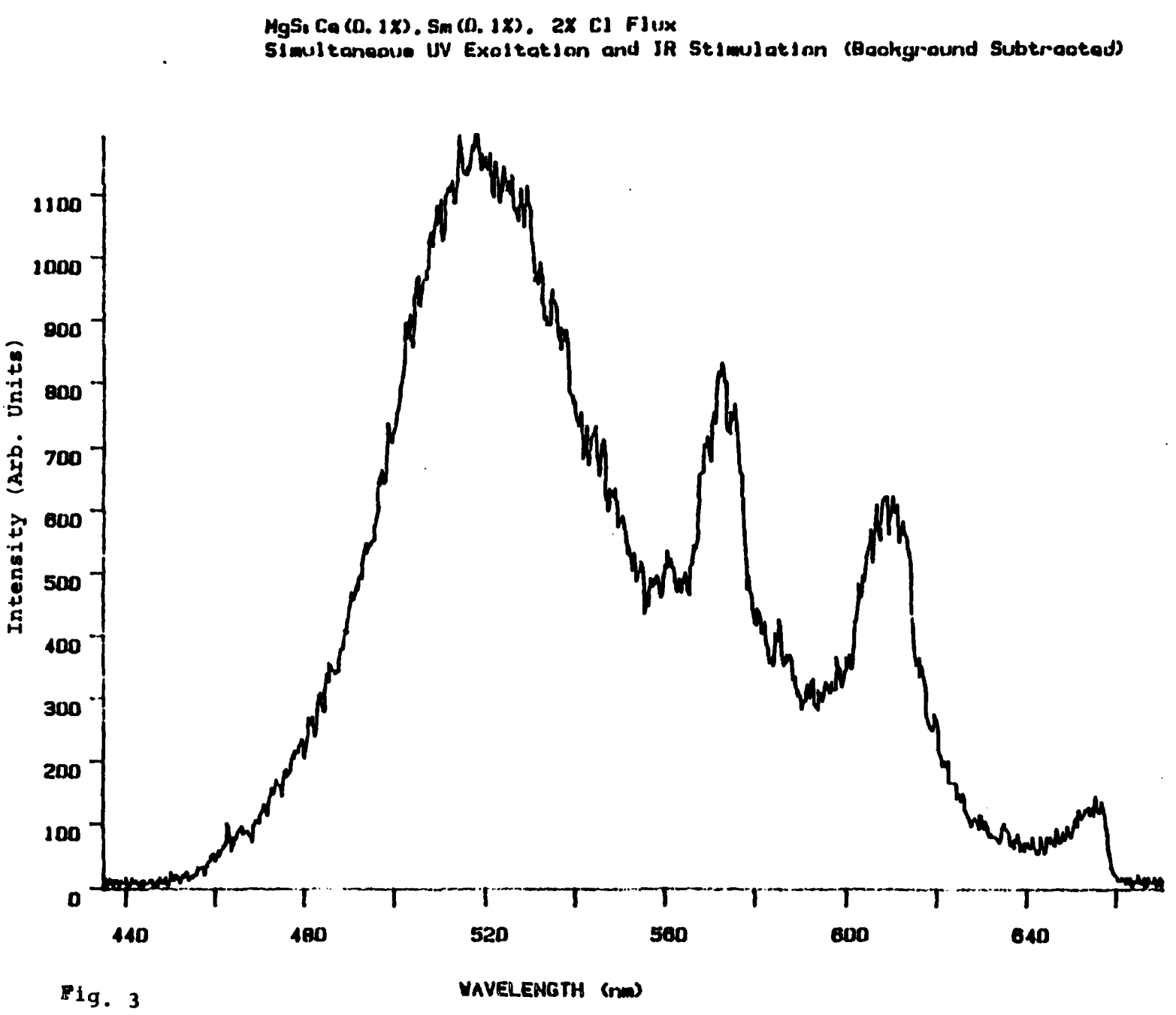
MgS: Ce(0.1%), Sm(0.1%), 2% Cl Flux
Simultaneous UV Excitation and IR Stimulation (Background Subtracted)
Intensity (Arb. Units)
0
100
200
300
400
500
600
700
800
900
1000
1100
440
480
520
560
600
640
WAVELENGTH (nm)

Fig. 3

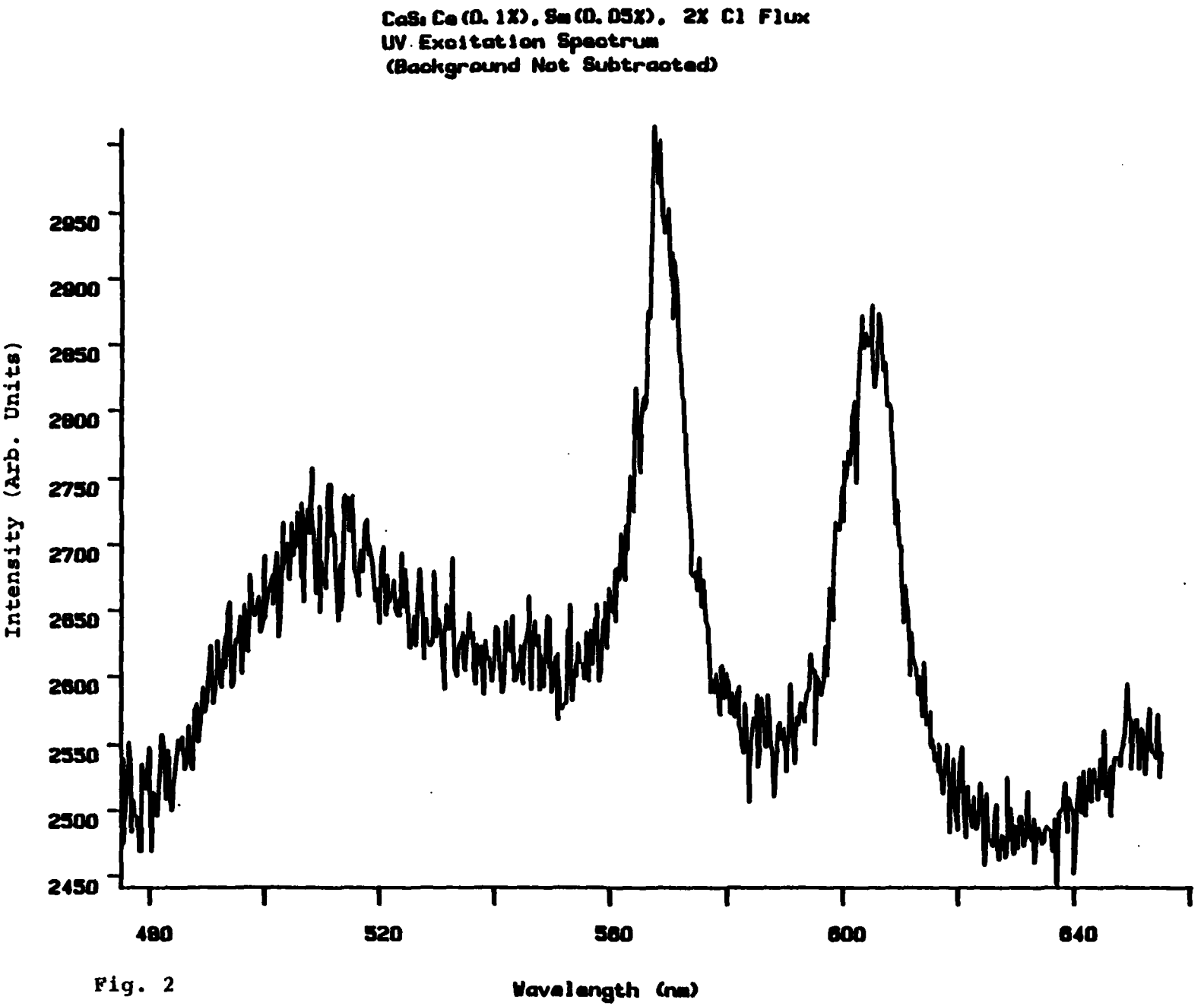
CaS:Ce(0.1%),Sm(0.05%), 2% Cl Flux
UV Excitation Spectrum
(Background Not Subtracted)
Intensity (Arb. Units)
2950
2900
2850
2800
2750
2700
2650
2600
2550
2500
2450
480
520
560
600
640
Wavelength (nm)

Fig. 2

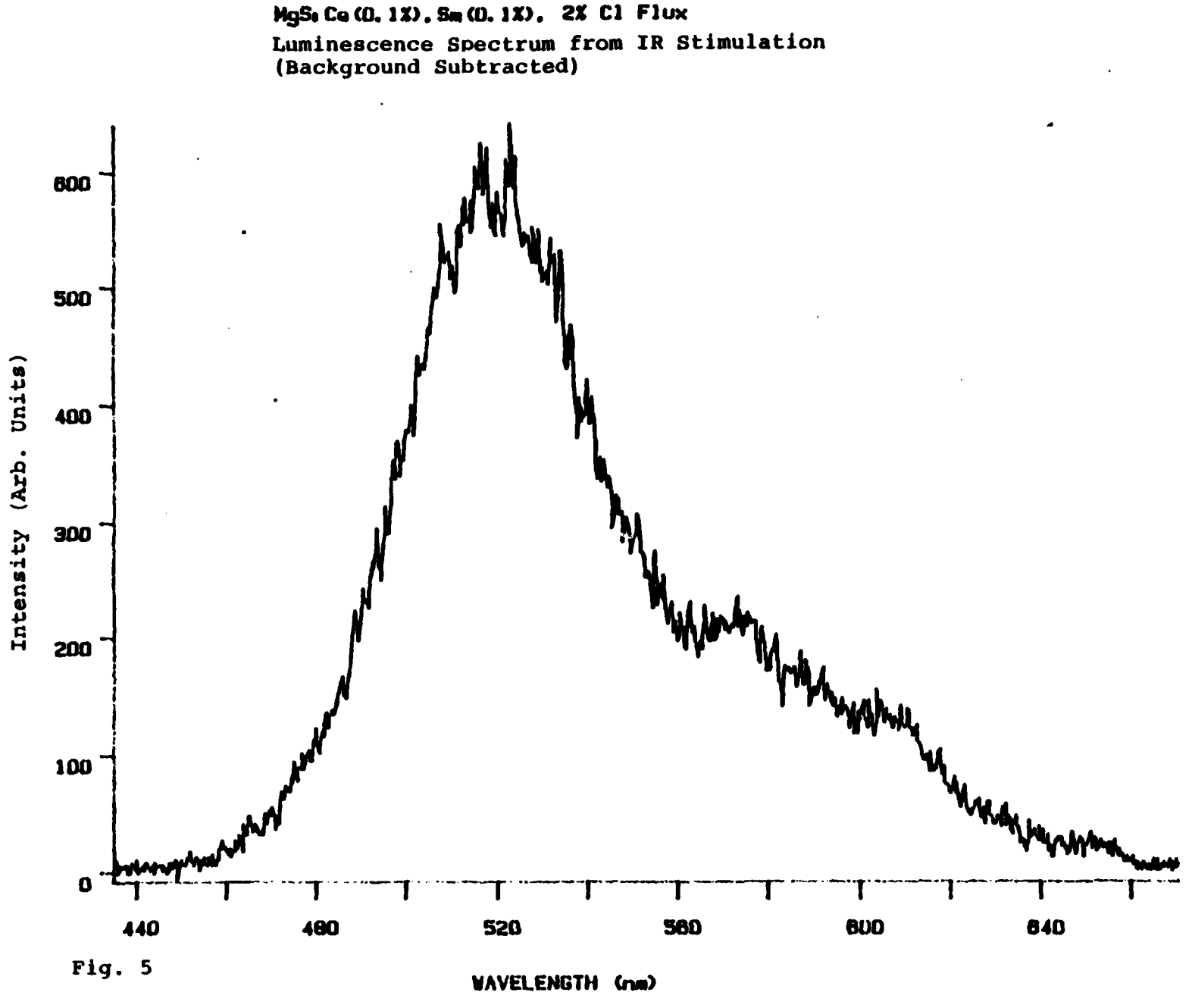
MgS: Ce (0.1%), Sm (0.1%), 2% Cl Flux
Luminescence Spectrum from IR Stimulation
(Background Subtracted)
Intensity (Arb. Units)
600
500
400
300
200
100
0
440
480
520
560
600
640
WAVELENGTH (nm)

Fig. 5

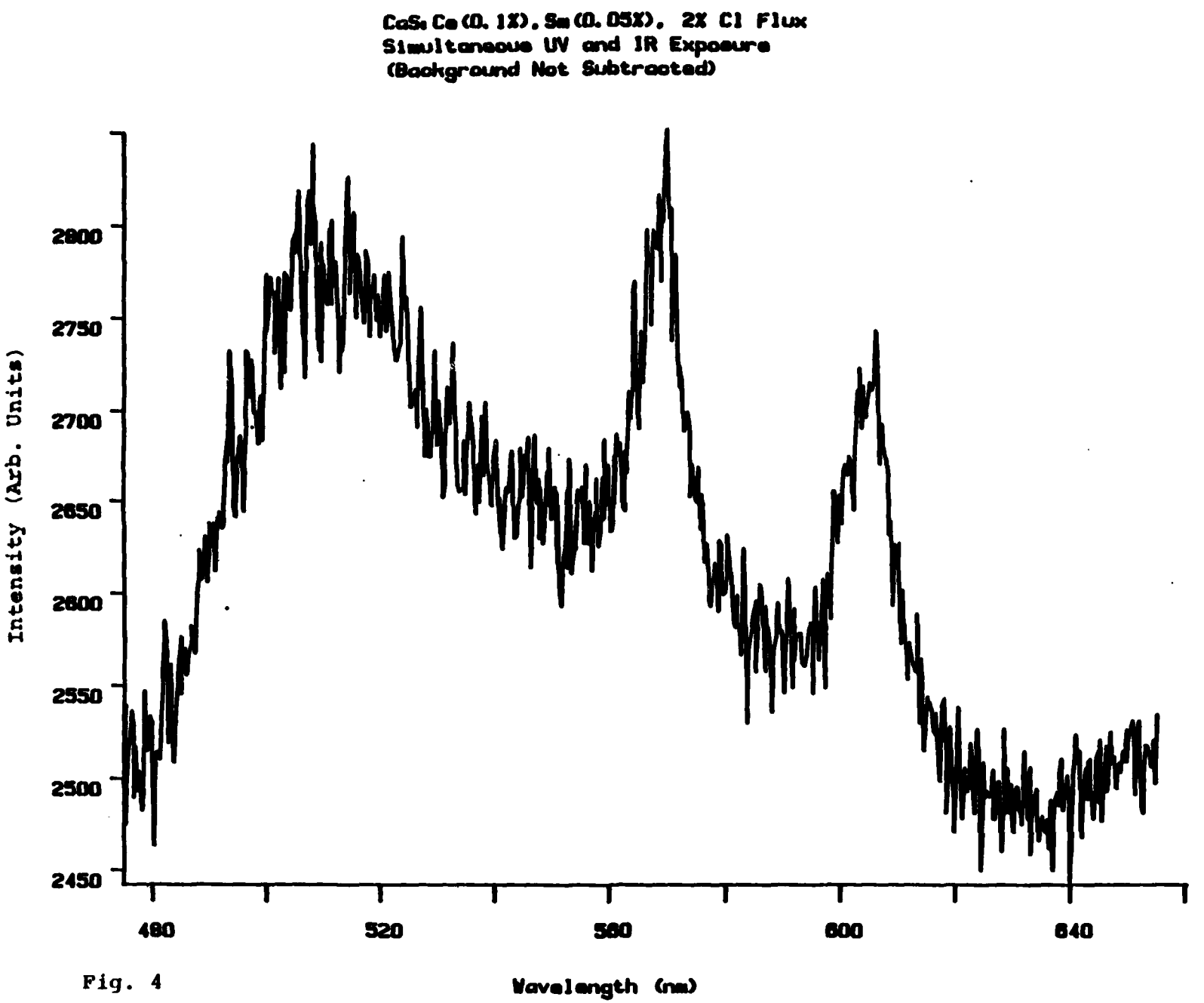
CaS:Ce(0.1%),Sm(0.05%), 2% Cl Flux
Simultaneous UV and IR Exposure
(Background Not Subtracted)
Intensity (Arb. Units)
2800
2750
2700
2650
2600
2550
2500
2450
480
520
560
600
640
Wavelength (nm)

Fig. 4

IR STIMULATION SPECTRUM

MAGNESIUM SULFIDE: CERIUM, SAMARIUM

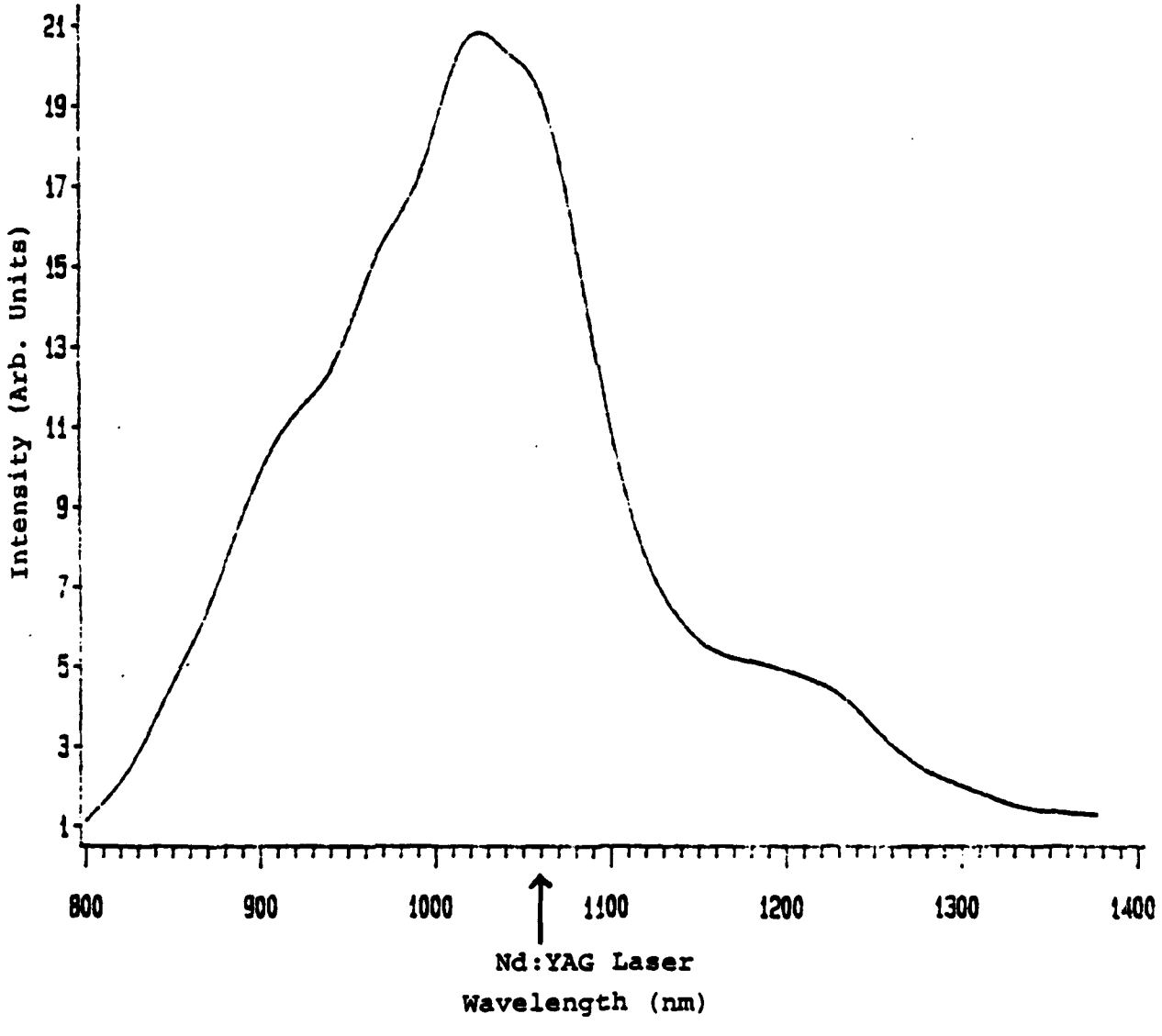

Fig. 7

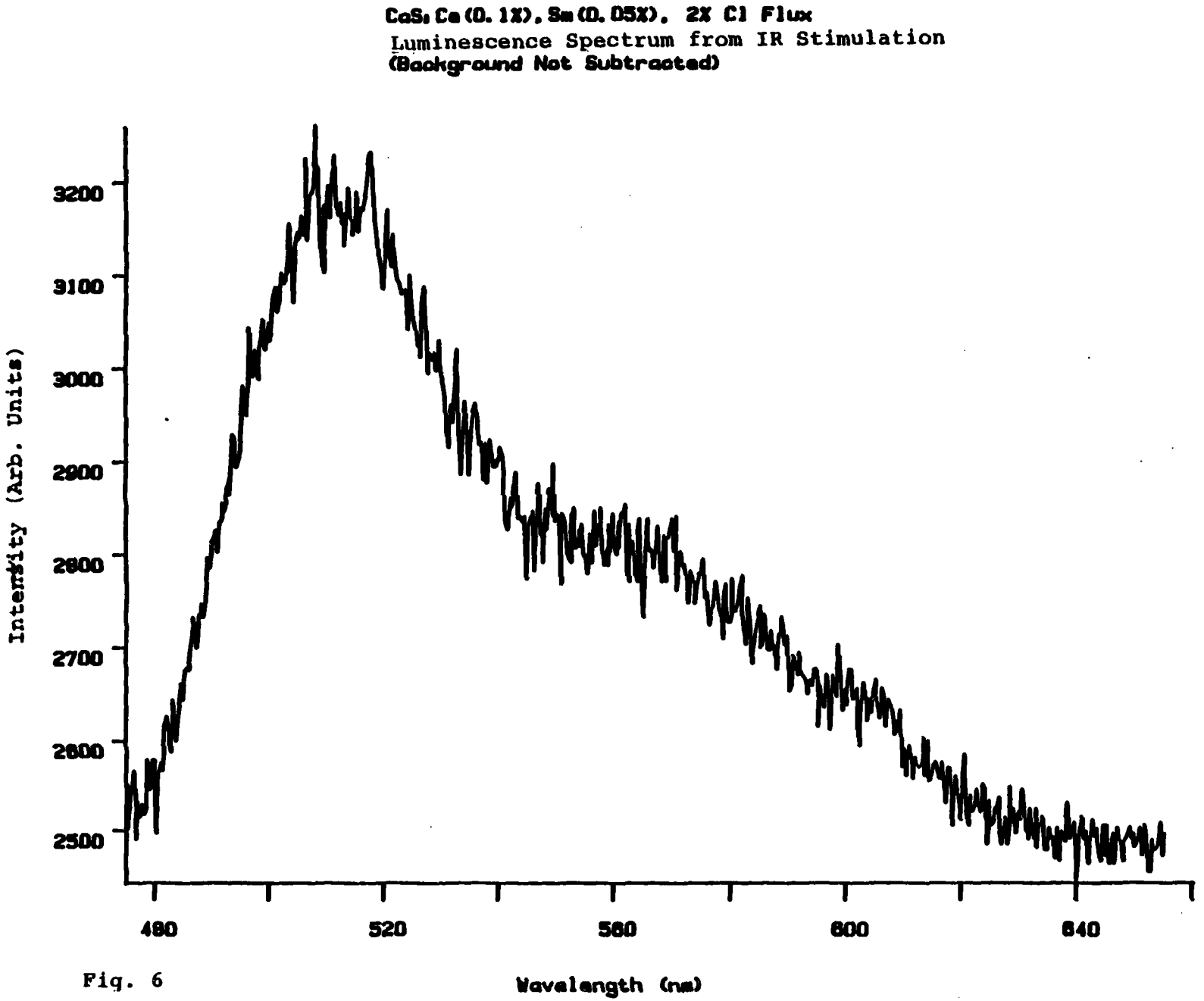
CaS:Ce(0.1%),Sm(0.05%), 2% Cl Flux
Luminescence Spectrum from IR Stimulation
(Background Not Subtracted)
Intensity (Arb. Units)
3200
3100
3000
2900
2800
2700
2600
2500
480
520
560
600
640
Wavelength (nm)

Fig. 6

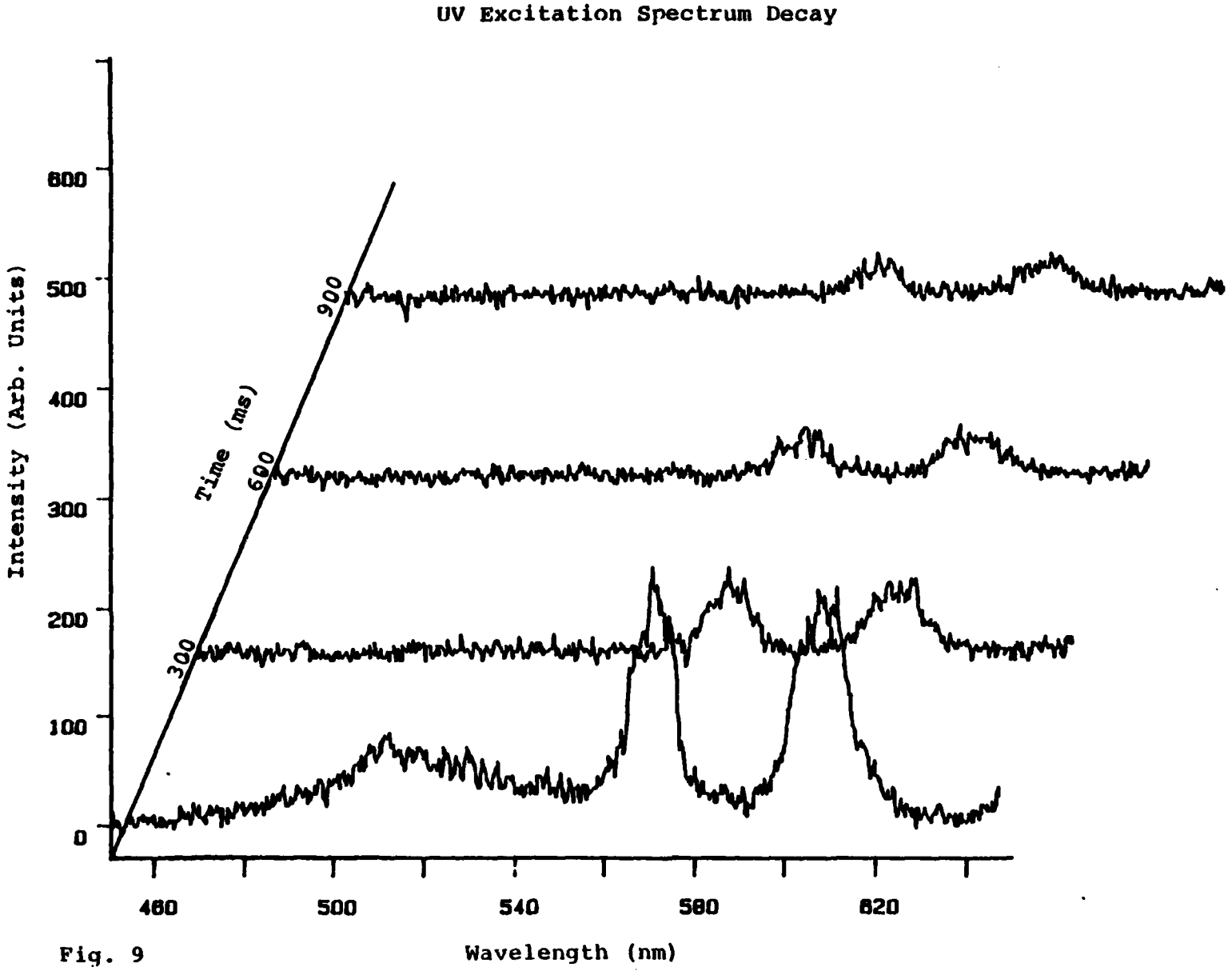
UV Excitation Spectrum Decay
Intensity (Arb. Units)
600
500
400
300
200
100
0
Time (ms)
900
600
300
460
500
540
580
620
Wavelength (nm)

Fig. 9

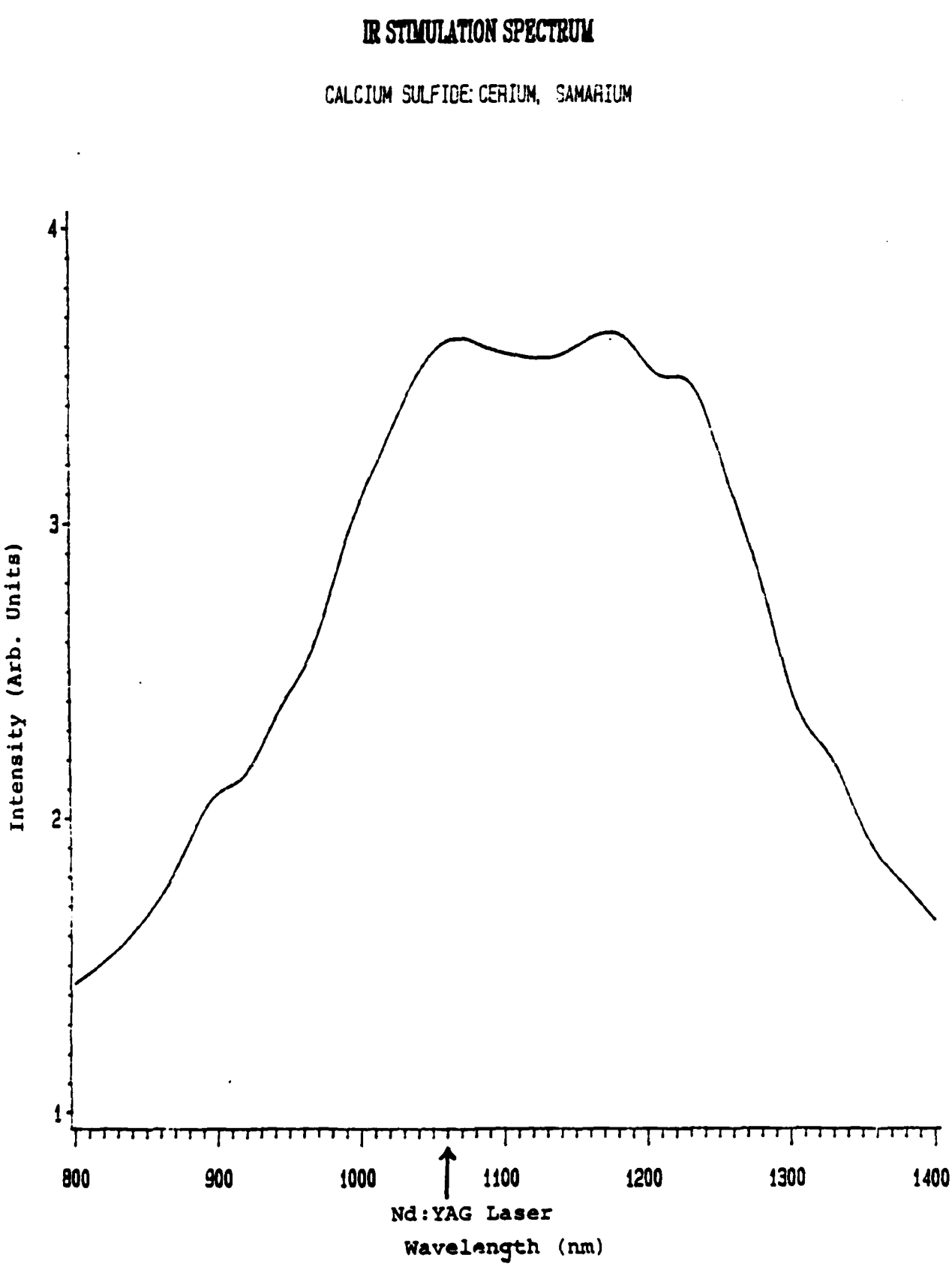
IR STIMULATION SPECTRUM
CALCIUM SULFIDE: CERIUM, SAMARIUM
Intensity (Arb. Units)
4
3
2
1
800
900
1000
1100
1200
1300
1400
Nd:YAG Laser
Wavelength (nm)

Fig. 8

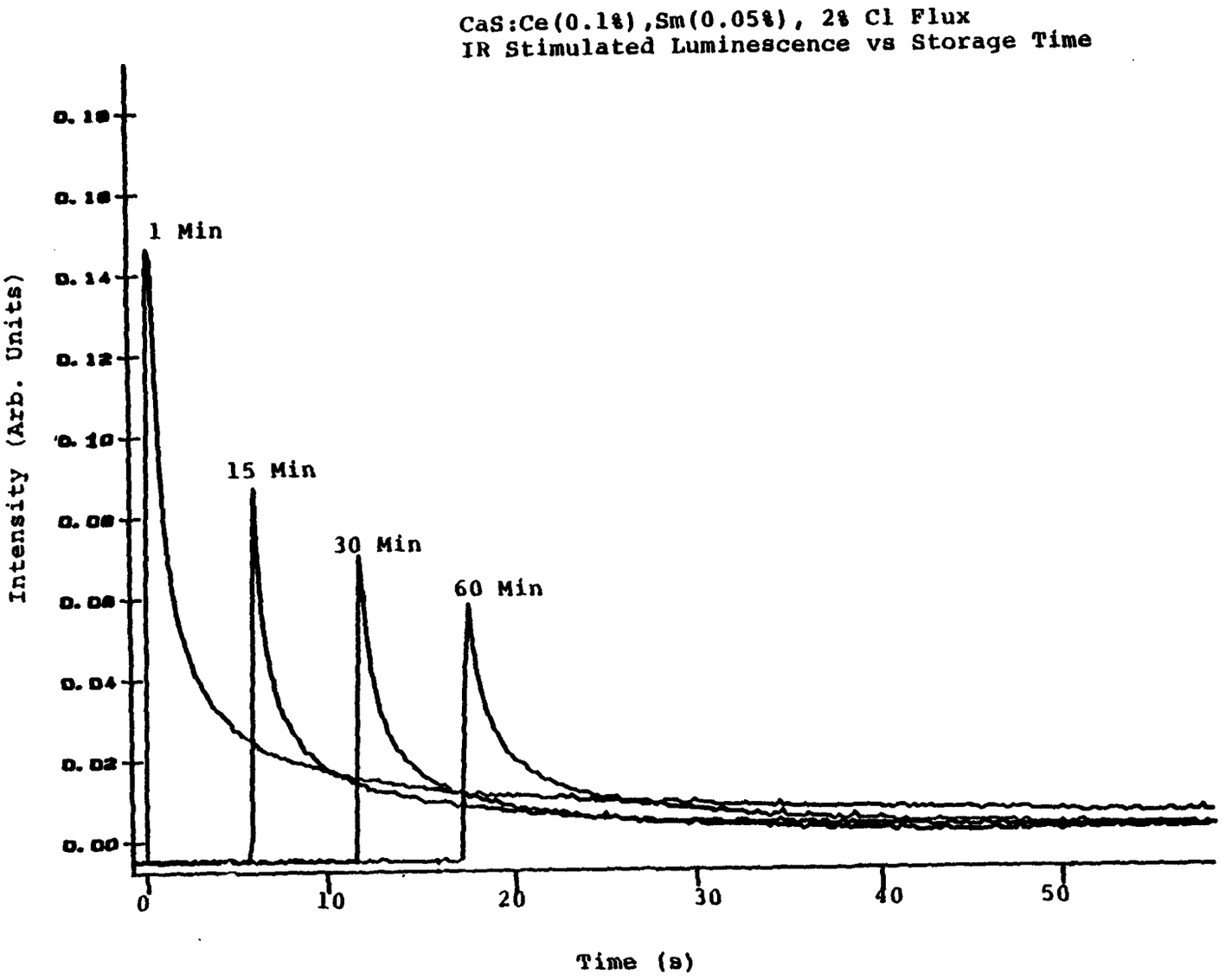
CaS:Ce(0.1%),Sm(0.05%), 2% Cl Flux
IR Stimulated Luminescence vs Storage Time
Intensity (Arb. Units)
0.16
0.14
0.12
0.10
0.08
0.06
0.04
0.02
0.00
1 Min
15 Min
30 Min
60 Min
0
10
20
30
40
50
Time (s)

Fig. 11

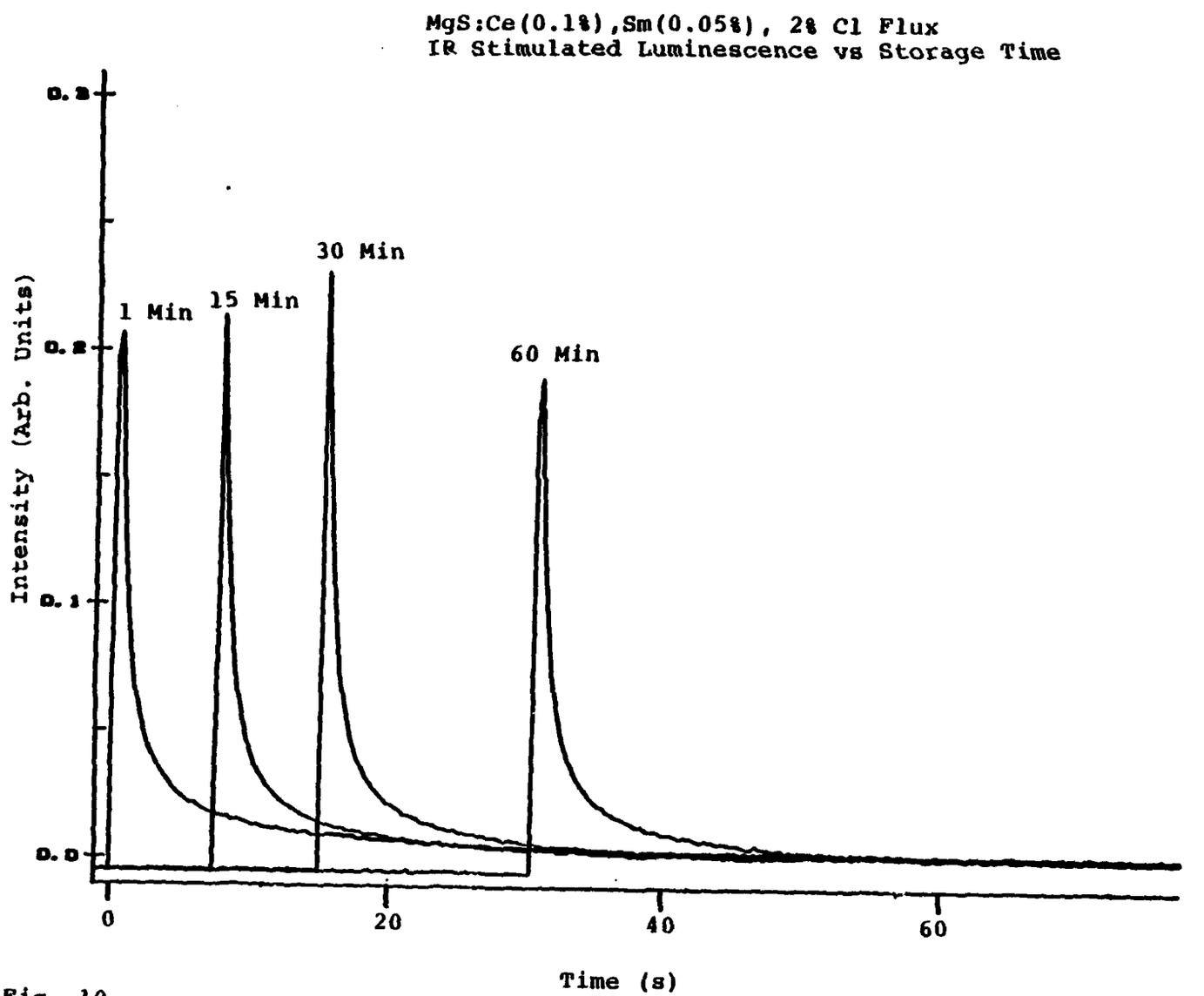
MgS:Ce(0.1%),Sm(0.05%), 2% Cl Flux
IR Stimulated Luminescence vs Storage Time
0.3
0.2
0.1
0.0
Intensity (Arb. Units)
1 Min
15 Min
30 Min
60 Min
0
20
40
60
Time (s)

Fig. 10

PAPERS SUBMITTED TO REFEREED JOURNALS:

1. "LASER-STIMULATED EXOELECTRON EMISSION"
by
P. Braunlich and P. Kelly
(Submitted to Japan. J. Appl. Physics on August 26, 1985)

2. "TRANSIENT TEMPERATURE RESPONSE OF A TWO-LAYER SYSTEM HEATED WITH A LOCALIZED LASER BEAM"
by
A. Abtahi, P. Braunlich, and P. Kelly
(Submitted to J. Appl. Phys., April 1986)

3. "LASER STIMULATED THERMOLUMINESCENCE II"
by
P. Kelly. A. Abtahi, and P. Braunlich
(Submitted to J. Appl. Phys., April 1986)

4. "INVESTIGATION OF THERMOLUMINESCENCE EFFICIENCIES AT HIGH LASER HEATING RATES"
by
A. Abtahi, P. Braunlich, T. Haugan, and P. Kelly
(Submitted to Radiation Protection Dosimetry, Dec. 85)

OFFICE OF NAVAL RESEARCH

PUBLICATIONS / PATENTS / PRESENTATIONS / HONORS REPORT

for

1 October 1984 through 1-April 1986

for

Contract N00014-82-K-0529

Project-Task Area No. RR011-07-01

Work Unit No. NR395-079

INVESTIGATION OF BASIC CHARACTERISTICS OF LASER HEATING IN THERMOLUMINESCENCE

Principle Investigator: Peter F. Braunlich

WASHINGTON STATE UNIVERSITY
DEPARTMENT OF PHYSICS
PULLMAN, WA 99164-2814

INVITED PRESENTATIONS AT TOPICAL OR SCIENTIFIC/TECHNICAL CONFERENCES:

"LASER STIMULATED EXOELECTRON EMISSION"

by

P. Braunlich and P. Kelly

INVITED PRESENTATION

8th International Symposium on Exoelectron Phenomena and Applications

AUGUST 25-29,1985

OSAKA, JAPAN

HONORS/AWARDS: NONE

BOOKS: NONE

PATENTS FILED: NONE

PATENTS GRANTED: NONE

PAPERS PUBLISHED IN REFEREED JOURNALS:

"LASER STIMULATED THERMOLUMINESCENCE"
by
A. Abtahi, P. Braunlich, P. Kelly, and G. Gasiot
J. Appl. Phys 58, pp. 1626-1639 (1985
This paper is a comprehensive report on laser heating in thermoluminescence using Gaussian laser beam profiles.

REPORTS DISTRIBUTION LIST FOR ONR PHYSICS DIVISION OFFICE
UNCLASSIFIED CONTRACTS

Director Defense Advanced Research Projects Agency Attn: Technical Library 1400 Wilson Blvd. Arlington, Virginia 22209	1 copy
Office of Naval Research Physics Division Office (Code 412) 800 North Quincy Street Arlington, Virginia 22217	2 copies
Office of Naval Research Director, Technology (Code 200) 800 North Quincy Street Arlington, Virginia 22217	1 copy
Naval Research Laboratory Department of the Navy Attn: Technical Library Washington, DC 20375	1 copy
Office of the Director of Defense Research and Engineering Information Office Library Branch The Pentagon Washington, DC 20301	1 copy
U.S. Army Research Office Box 1211 Research Triangle Park North Carolina 27709	2 copies
Defense Technical Information Center Cameron Station Alexandria, Virginia 22314	12 copies
Director, National Bureau of Standards Attn: Technical Library Washington, DC 20234	1 copy
Director U.S. Army Engineering Research and Development Laboratories Attn: Technical Documents Center Fort Belvoir, Virginia 22060	1 copy
ODDR&E Advisory Group on Electron Devices 201 Varick Street New York, New York 10014	1 copy

Naval Ordnance Station — 1 copy
Technical Library
Louisville, Kentucky 40214

Commanding Officer — 1 copy
Naval Ocean Research & Development Activity
Technical Library
NSTL Station, Mississippi 39529

Naval Explosive Ordnance Disposal Facility — 1 copy
Technical Library
Indian Head, Maryland 20640

Naval Ocean Systems Center — 1 copy
Technical Library
San Diego, California 92152

Naval Surface Weapons Center — 1 copy
Technical Library
Silver Spring, Maryland 20910

Naval Ship Research and Development Center — 1 copy
Central Library (Code L42 and L43)
Bethesda, Maryland 20084

Naval Avionics Facility — 1 copy
Technical Library
Indianapolis, Indiana 46218

Air Force Office of Scientific Research — 1 copy
Department of the Air Force
Bolling AFB, DC 22209

Air Force Weapons Laboratory — 1 copy
Technical Library
Kirtland Air Force Base
Albuquerque, New Mexico 87117

Air Force Avionics Laboratory — 1 copy
Air Force Systems Command
Technical Library
Wright-Patterson Air Force Base
Dayton, Ohio 45433

Lawrence Livermore Laboratory — 1 copy
Attn: Dr. W. F. Krupke
University of California
P.O. Box 808
Livermore, California 94550

Harry Diamond Laboratories — 1 copy
Technical Library
2800 Powder Mill Road
Adelphi, Maryland 20783

Naval Air Development Center — 1 copy
Attn: Technical Library
Johnsville
Warminster, Pennsylvania 18974

Naval Weapons Center — 1 copy
Technical Library (Code 753)
China Lake, California 93555

Naval Underwater Systems Center — 1 copy
Technical Center
New London, Connecticut 06320

Commandant of the Marine Corps — 1 copy
Scientific Advisor (Code RD-1)
Washington, DC 20380

Naval Ordnance Station — 1 copy
Technical Library
Indian Head, Maryland 20640

Naval Postgraduate School — 1 copy
Technical Library (Code 0212)
Monterey, California 93940

Naval Missile Center — 1 copy
Technical Library (Code 5632.2)
Point Mugu, California 93010

Naval Ordnance Station — 1 copy
Technical Library
Louisville, Kentucky 40214

Commanding Officer — 1 copy
Naval Ocean Research & Development Activity
Technical Library
NSTL Station, Mississippi 39529

Naval Explosive Ordnance Disposal Facility — 1 copy
Technical Library
Indian Head, Maryland 20640

Naval Ocean Systems Center — 1 copy
Technical Library
San Diego, California 92152

Naval Surface Weapons Center — 1 copy
Technical Library
Silver Spring, Maryland 20910

Naval Ship Research and Development Center — 1 copy
Central Library (Code L42 and L43)
Bethesda, Maryland 20084

Naval Avionics Facility — 1 copy
Technical Library
Indianapolis, Indiana 46218

END

FILMED

5-86

DTIC